Rivista Italiana di Paleontologia e Stratigrafia	volume 101	numero 3	tavole 1-4	pagine 267-300	Dicembre 1995

TRIASSIC OF SPITI (TETHYS HIMALAYA, N INDIA)

EDUARDO GARZANTI, FLAVIO JADOUL, ALDA NICORA & FABRIZIO BERRA

Key-words: Triassic, Biostratigraphy, Ammonoids, Conodonts, Foraminifers, Sequence stratigraphy, Sea-level changes.

Riassunto. Le successioni esposte nelle Valli di Pin e Spiti, un'area classica per il Triassico della Tetide, forniscono una registrazione sedimentaria e paleontologica straordinariamente completa, ideale per verificare la validità delle carte eustatiche globali e l' applicabilità dei moderni concetti di stratigrafia sequenziale.

Il limite Permiano/Triassico corrisponde a una importante lacuna, soprattutto nell' alta valle di Pin dove l' interruzione della sedimentazione si è prolungata per diversi Ma. Nello Scitico e nell' Anisico, la Formazione di Tamba Kurkur registra una serie di fluttuazioni eustatiche, con sedimentazione condensata di calcari nodulari pelagici sulla piattaforma continentale esterna e sull'inizio della scarpata durante le fasi trasgressive, e deposizione di peliti di piattaforma nelle fasi regressive. Un livello condensato a glauconia cade circa al limite Anisico/Ladinico, e il tetto della formazione raggiunge il Ladinico basale nelle sezioni più prossimali e complete.

Il tardo Ladinico inferiore segna un aumento del detrito terrigeno fine, ma i tassi di accumulo rimangono bassi per la parte inferiore del Gruppo di Hanse, per aumentare bruscamente nella parte centrale del Carnico, raggiungendo i 100 m/Ma alla fine del piano.

Almeno nove sequenze transgressivo/regressive di III o IV ordine sono distinguibili nella Formazione di Nimaloksa e nel Gruppo di Alaror, dove la distribuzione delle facies indica che il margine continentale passivo indiano si approfondiva verso nord. La Formazione di Nimaloksa documenta la progradazione di una rampa carbonatica nel Carnico sommitale (Membro Inferiore), seguita nel Norico inferiore dalla sedimentazione subtidale mista carbonatico/terrigena del Membro Medio e poi dai depositi di piattaforma carbonatica del Membro Superiore. La discordanza erosiva alla base del Gruppo di Alaror registra quindi un evento tettonico distensivo, seguito dal rapido aumento del detrito quarzoso-feldspatico nel tardo Norico inferiore. Gli apporti terrigeni si riducono solo durante i picchi trasgressivi, segnati da orizzonti condensati a ooliti ferruginose o fosfati e, attorno al limite Norico inferiore/Norico medio, dalla crescita in acque più pulite di piccole biocostruzioni ("Coral limestone"). I tassi di accumulo iniziano a ridursi progressivamente prima della fine del Triassico, quando un' unità arenacea più grossolana ("Quartzite series") segna una importante regressione, subito seguita da una grande trasgressione alla base del Gruppo di Kioto.

Abstract. The successions exposed in the Pin and Spiti valleys, a classical area for the Tethyan Triassic, provides an extraordinarily complete sedimentary and paleontologic record and is thus well-suited to check the validity of global eustatic charts and applicability of sequence stratigraphic concepts. New detailed stratigraphic data allowed us to present a revised lithostratigraphic scheme - largely based on previous works by Hayden (1904) and Srikantia (1981) - which can be directly compared with successions exposed all along the Tethys Himalaya from Zanskar to Tibet.

The Permian/Triassic boundary represents a major break in sedimentation, with time gaps of up to several Ma testified in the upper Pin valley. In the Induan to Anisian, the Tamba Kurkur Fm. mainly documents global eustatic changes, with transgressive stages characterized by sedimentation of condensed nodular limestones on the outermost shelf/uppermost slope (e.g., Griesbachian/Early Dienerian, Spathian) and regressive stages marked by mudrock deposition on the continental shelf (e.g., Late Dienerian/Smithian). A glauconitic condensed horizon occurs at the Anisian/Ladinian boundary, and the top of the formation reaches the Early Ladinian in more complete proximal sections.

Greater clay supply characterizes the late Early Ladinian, but accumulation rates remain low in the lower part of the Hanse Group (Kaga and Chomule Fms.), to increase sharply in the late Early to early Late Carnian ("Grey beds"), reaching 100 m/Ma in the latest Carnian (Nimaloksa Fm.).

At least nine, third- to fourth-order transgressive/regressive sequences can be recognized in the Nimaloksa Fm. and Alaror Group, where facies distribution patterns indicate that the Spiti continental margin deepened towards the north. The Nimaloksa Fm. documents progradation of a carbonate ramp in the latest Carnian (Lower Member), followed in the Early Norian by subtidal mixed carbonate/terrigenous sedimentation (Middle Member) and by platform carbonate deposits (Upper Member). Next, the major disconformity at the base of the Alaror Group testifies to an extensional tectonic event, followed by rapid increase in quartzo-feldspathic detritus in the late Early Norian. Siliciclastic supply is reduced only during flooding stages, marked by oolitic ironstone or phosphatic condensed horizons ("*Juvavites* beds", "*Monotis* shale"); cleaner waters foster local development of knoll reefs around the Early/Middle Norian boundary ("Coral limestone"). Accumulation rates gradually begin to decrease before the close of the Triassic, when the "Quartzite series" records a sharp regressive event, followed by renewed transgression at the base of the Kioto Group.

Introduction.

The Triassic sedimentary succession of Spiti has been the subject of classical stratigraphic studies for over a century (Fig. 1). Complete sections from the top of the Permian to the base of the Jurassic, from 1150 to

- Dipartimento di Scienze della Terra, Università degli Studi, Via Mangiagalli 34, 20133 Milano (Italia) - Ev-K2-CNR, Via Ampère 56, 20133 Milano (Italia).

Con il parziale contributo del Progetto Coordinato CNR "Ritmi ed Eventi in Biostratigrafia" (Coord.: prof. A. Farinacci) - Sottoprogetto "Microfossili ed Eventi Paleozoici" (Resp. Sci.: prof. M. Tongiorgi).

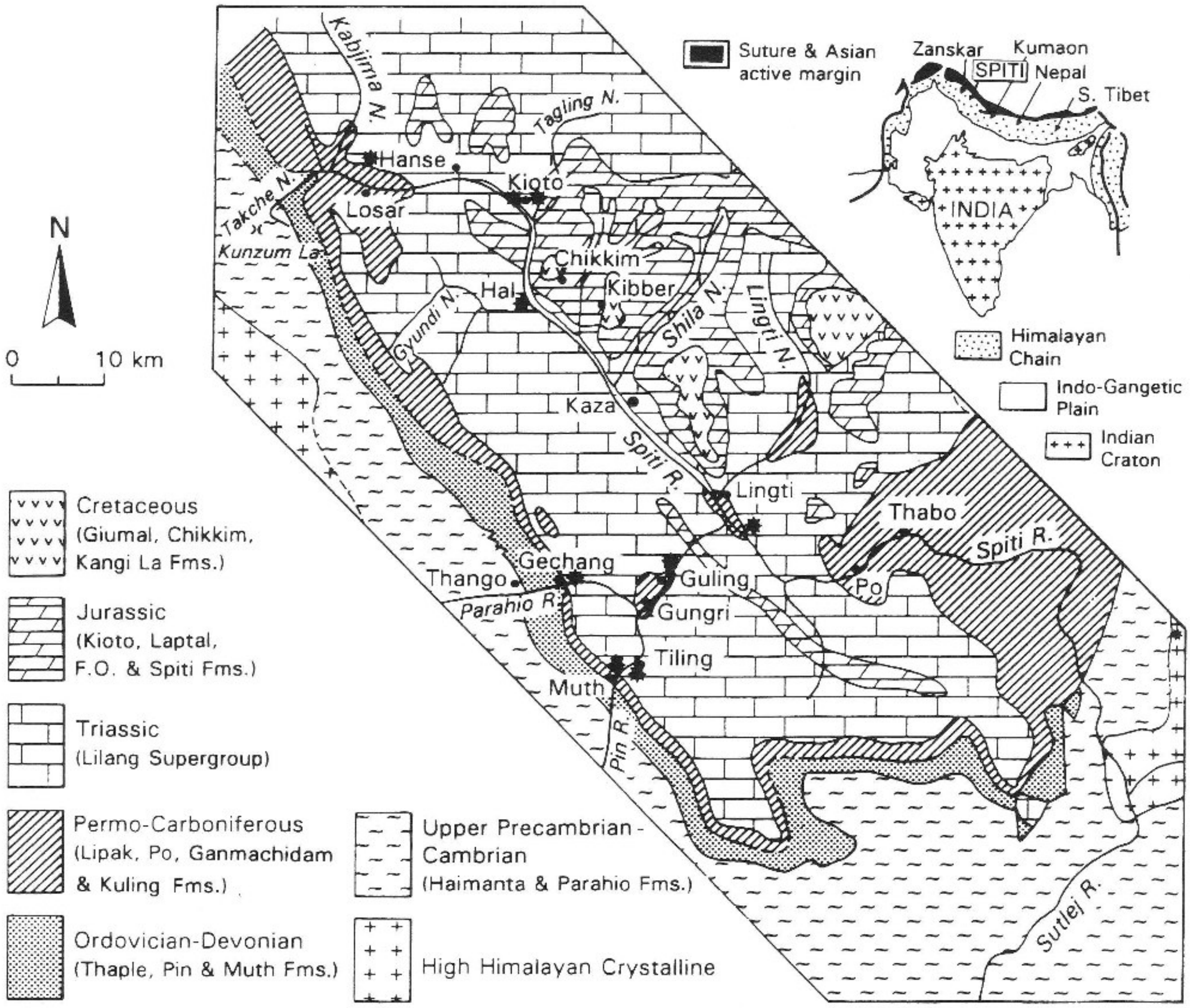

Fig. 1 - Geological sketch map of the Spiti river valley, from Kunzum La to confluence with the Sutlej river (after Hayden, 1904; Bagati, 1990). Geographic position of localities cited in text is shown; asterisks indicate location of measured sections.

1200 m in thickness, can be measured without losing a bed in the upper Pin valley (Muth). Good reference sections are exposed in the Tiling-Gechang-Guling area to the north and in the upper Spiti valley between Losar and Kioto, where the Triassic reaches 1300 m in thickness overall. Ammonoids and conodonts, found in many intervals, represent excellent biostratigraphic check-points from the base of the Triassic to the Middle Norian. Spiti thus represents one of the most interesting areas in the world for detailed stratigraphic studies on the Tethyan Triassic, and to check the validity of global eustatic charts and applicability of modern sequence stratigraphy concepts.

The purpose of the present paper, which is the result of a continuing research project on the paleogeographic evolution of the Tethys Himalayan Zone carried out at the University of Milan, is to provide a wealth of new detailed stratigraphic data along with a synthesis of current knowledge on the Triassic stratigraphy of Spiti. Over 250 samples for petrographic and paleontological analysis were collected in 14 detailed stratigraphic sections measured during the summer 1992 geological expedition. The earlier lithostratigraphic nomenclature is revised herein, and a simple general scheme is proposed, which is based on our data and observations but also on the many previous works dealing with the Zanskar-Spiti Synclinorium (e.g., Hayden, 1904; Diener, 1908, 1912; Srikantia et al., 1980; Srikantia, 1981; Fuchs, 1982; Bhargava, 1987; Bagati, 1990).

Given the relative homogeneity of Triassic sedimentary units all along the Tethys Himalayan Zone, this framework can be directly compared not only with the adjacent Zanskar region (Nicora et al., 1984; Jadoul et al., 1990; Gaetani & Garzanti, 1991), but also with the Triassic stratigraphy of central Nepal (Garzanti et al., 1992, 1994a) and even southern Tibet (Jadoul et al.,

	SPITI Hayden 1904	SPITI Srikantia 1981		SPITI Fuchs 1982		SPITI Bhargava 1987		ZANSKAR Gaetani et al. 1986 Jadoul et al. 1990		SPITI This paper
	Megalodon limestone 700 m	SIMOKHAMBDA Formation 750 m		KIOTO Limestone		KIOTO Formation 700 m		KIOTO Limestone 480 - 550 m		KIOTO Group > 600 m
	Quarzite series 100 m	ALAROR Formation 100 m		Quartzite Series 50 - 100 m		NUNULUKA Formation 100 m	QUARTZITE SERIES	Member c 43 -70 m	ALAROR GROUP	Quartzite series 15 - 35 m
	Monotis shales 90 m		250 - 300 m	Monotis Shales		ALAROR Formation 90 m		Member b 42 - 94 m		Monotis shale 120 - 160 m
	Coral limestone 30 m			Coral Limestone 0 - 300 m		HANGRANG Formation 20 m				Coral limestone 15 - 20 m
	Juvavites beds 150 m			Juvavites Shales	SANGLUNG FORMATION	Member C 180 m		Member a 54 - 97 m		Juvavites beds 110 - 195 m
TROPITES BEDS	dolomitic limestone 90 m	NIMALOKSA Formation 300 m	TROPITES LST.	limestones & dolostones ~ 120 m		Member B 265 m		ZOZAR Formation 157 - 168 m	NIMALOKSA FM.	Upper Member 105 - 160 m
	limestone & shale 65 m			limestones, marls, sandstones & shales ~80 m			HANSE FORMATION	upper member 275 m		Middle Member 170 - 205 m
	brachiopod limestone 120 m			limestone with shales ~80 m						Lower Member 160 m
	Grey beds 165 m	HANSE Formation 350 m		Grey beds 175 - 225 m		Member A 195 m			HANSE GROUP	Grey beds 205 m
	Halobia limestone 40 m			Halobia / Daonella Limestone 80 - 90 m	CHOMULE FM.	Halobia beds 35 m		?		CHOMULE Formation 85 - 100 m
	Daonella limestone 45 m					Daonella Limestone ~ 50 m		middle member 170 m		
	Daonella shales 50 m			Daonella Shales 45 - 55 m	KAGA FM.	Daonella Shale ~ 50 m		lower member 70 m		KAGA Formation 42 - 60 m
LOWER TRIAS	Upper & Lower Muschelkalk 8 m	TAMBA KURKUR Formation 500 m		SCYTHO - ANISIAN 30 m	MIKIN FORMATION	Upper & Lower Muschelkalk 8 m	TAMBA KURKUR FM.	upper member 10 - 20 m	TAMBA KURKUR FM.	Muschelkalk 5 - 7 m
	Nodular limestone 18 m					Nodular Limestone 18 m		middle member 5 - 15 m		Nodular limestone 14 - 21 m
	Horizons of *R. griesbachi* & *P. himalca* 2 m					Basal Muschelkalk ~ 1 m		lower member 20 m		Hedenstroemia beds 13 - 25 m
	Hedenstroemia beds 10 m					Hedenstroemia Beds 7 m				
	Meekoceras zone Ophiceras zone Otoceras zone 2 m					Meekoceras zone Ophiceras zone Otoceras zone ~ 4 m				First limestone band 0 - 1 m

Tab. 1 - Triassic lithostratigraphy for the Tethys Himalaya of Spiti. Nomenclature proposed in the present paper is compared with that adopted by previous research teams in Spiti and Zanskar.

1995). Further biostratigraphic information on the Spiti succession is contained in several other articles (e.g., Goel, 1977; Bhargava & Bassi, 1985; Bhargava & Gadhoke, 1988).

Adopted conodont zones are according to Matsuda (1985), Sweet (1988 a,b) and Kozur (1989a). Given accumulation rates are gross average figures based on the Haq et al. (1988) time scale; for the sake of simplicity compaction processes are not taken into account.

The Lilang Supergroup.

The new lithostratigraphic scheme proposed herein (Tab. 1) primarily results from an integration of the pioneering work by Hayden (1904) and the formal nomenclature of Srikantia (1981; Srikantia et al., 1980); some of the terms given by Bhargava (1987) are also adopted. For the sake of simplicity, no new formational name is introduced, whilst several terms are judged useless and are eliminated. The stratigraphic scheme previously proposed for Zanskar (Baud et al., 1984; Gaetani et al., 1986; Jadoul et al., 1990) is also emended.

The Lilang Group (Hayden, 1908), comprising all of the Triassic with the exception of the Rhaetian base of the Kioto Limestone (Baud et al., 1984; Gaetani et al., 1986; Bagati, 1990) is here elevated to supergroup rank. The *Lilang Supergroup* (Fig. 2) begins with the *Tamba Kurkur Formation* (Srikantia, 1981), a marker nodular limestone interval which can be traced all along the Tethys Himalaya from Zanskar (Srikantia et al., 1980; Nicora et al., 1984) to southern Tibet (Garzanti et al., 1995). The term Mikin Formation (Bhargava, 1987) is a junior synonym, and should be abandoned.

The Hanse Formation (Srikantia, 1981), here elevated to group rank, designates the overlying shelf marls and marly limestones in the Spiti-Zanskar Synclinorium (Srikantia et al., 1980; Gaetani et al., 1986). In Spiti, the *Hanse Group* includes the *Kaga Formation* (Bhargava, 1987; "Daonella shales" of Hayden, 1904), the *Chomule Formation* (Bhargava, 1987; "Daonella limestone" and "Halobia limestone" of Hayden, 1904) and the "*Grey beds*" (Hayden, 1904; Fuchs, 1982).

The overlying carbonates with intercalated terrigenous intervals have been named *Nimaloksa Formation* in the upper Spiti valley (Srikantia, 1981; "Tropites beds" of Hayden, 1904). The term Sanglung Formation (Bhargava, 1987) should be abandoned, since such a unit would include the "Grey beds", the whole of the Nimaloksa Fm., and the overlying "*Juvavites* beds" as well.

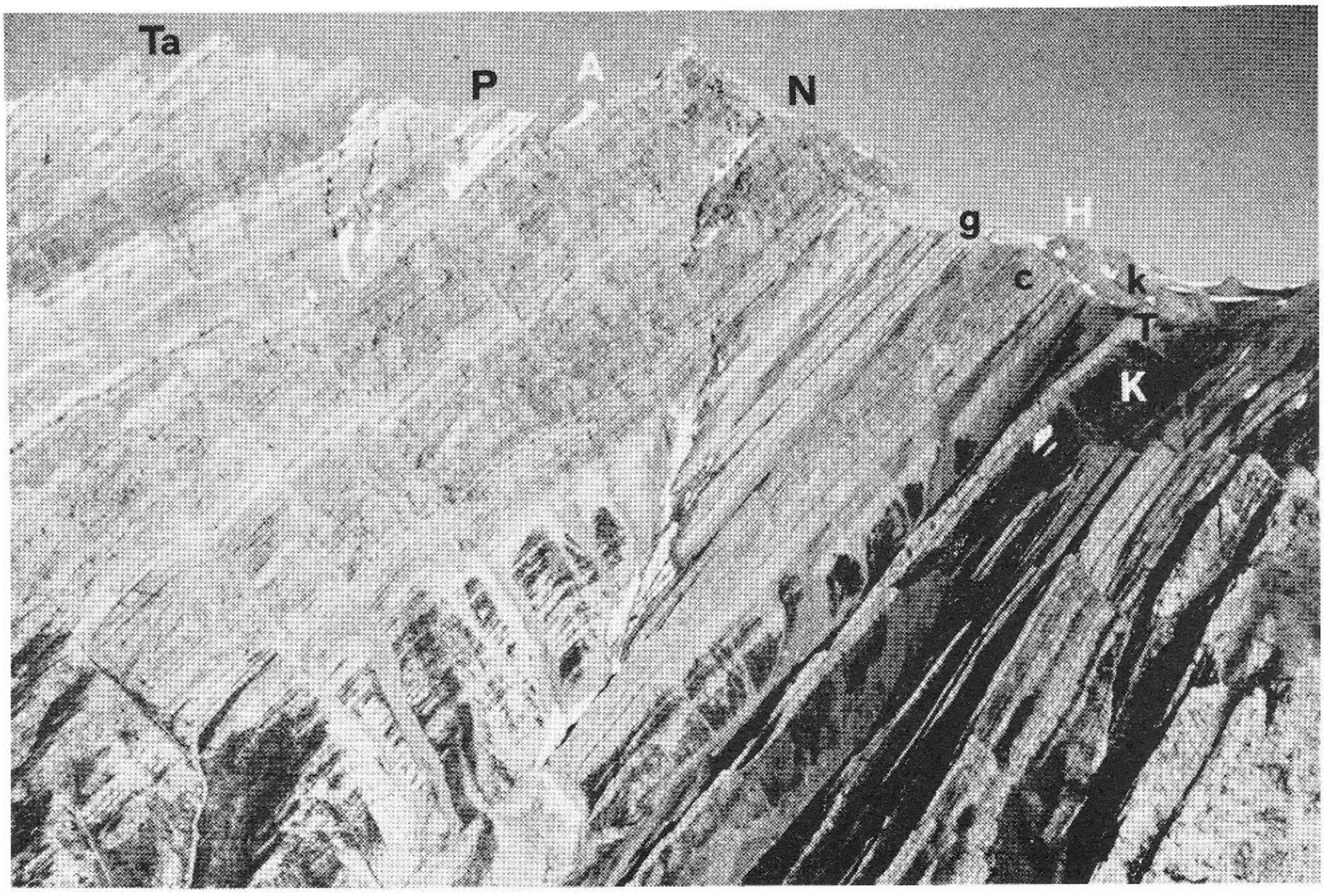

Fig. 2 - The Triassic succession in the Pin and upper Spiti valleys. Lilang Supergroup, spectacularly and continuously exposed at Muth, from Upper Permian Kuling Group (K) to Lower Jurassic Tagling Limestone (Ta) (T= Tamba Kurkur Fm.; H= Hanse Group: k= Kaga Fm., c= Chomule Fm., g= Grey beds; N= Nimaloksa Fm.; A= Alaror Group; P= Para Limestone).

A major unconformity marks the base of the Alaror Formation (Srikantia, 1981), here elevated to group rank. The unit was also recognized in Zanskar (Srikantia et al., 1980), where it has been improperly named "Quartzite series" (Baud et al., 1984; Jadoul et al., 1990; see Fuchs, 1987, p. 477). The *Alaror Group* includes four mixed terrigenous/carbonate units (*"Juvavites beds"*, *"Coral limestone"*, *"Monotis shale"* and *"Quartzite series"*; Hayden, 1904). The reasons why we prefer to use such informal names loosely, rather than the formal terms Hangrang Fm. (i.e., "Coral limestone") and Nunuluka Fm. (i.e., "Quartzite series") proposed by Bhargava (1987), is given below. Use of the term Alaror Fm. as an equivalent of the "*Monotis* shale" alone (Bhargava, 1987) should stop.

The Alaror Group is overlain, all along the Tethys Himalaya from Zanskar to Nepal and southern Tibet (Jadoul et al., 1990, 1995; Garzanti et al., 1992, 1994a), by the platform carbonates of the *Kioto Group*, of Rhaetian to mid-Dogger age (Diener, 1908; Jadoul & Sartorio, 1990); the Simokhambda Fm. of Srikantia (1981) is a much younger synonym. Only the Rhaetian lower part of the Kioto Group (*Para Limestone*; Stoliczka, 1866; Jadoul et al., 1990; "Megalodon limestone" of Hayden, 1904) will be dealt with in our paper.

Lithostratigraphy and biostratigraphy

Tamba-Kurkur Formation.

The Tamba Kurkur Fm. (Fig. 3; 36.3 m at Muth; 33.3 m at Guling; 54.2 m at Losar) unconformably overlies the Upper Permian black shales of the Gungri Formation (Garzanti et al., in prep.). The formation is here subdivided into four members (Fig. 4), largely retaining the subdivisions introduced by Hayden (1904): a basal limestone of Early Griesbachian to Early Dienerian age (*First limestone band*), is followed by thinner limestones and mudrocks of Late Dienerian to Late Smithian age (*"Hedenstroemia beds"*), and then by a resistant marker band of amalgamated limestones of latest Smithian to earliest Aegean age (*"Nodular limestone"*); the topmost member (*"Muschelkalk"*) consists of limestones and intercalated marls of Anisian to Early Ladinian age. A similar subdivision may hold at least in part for the adja-

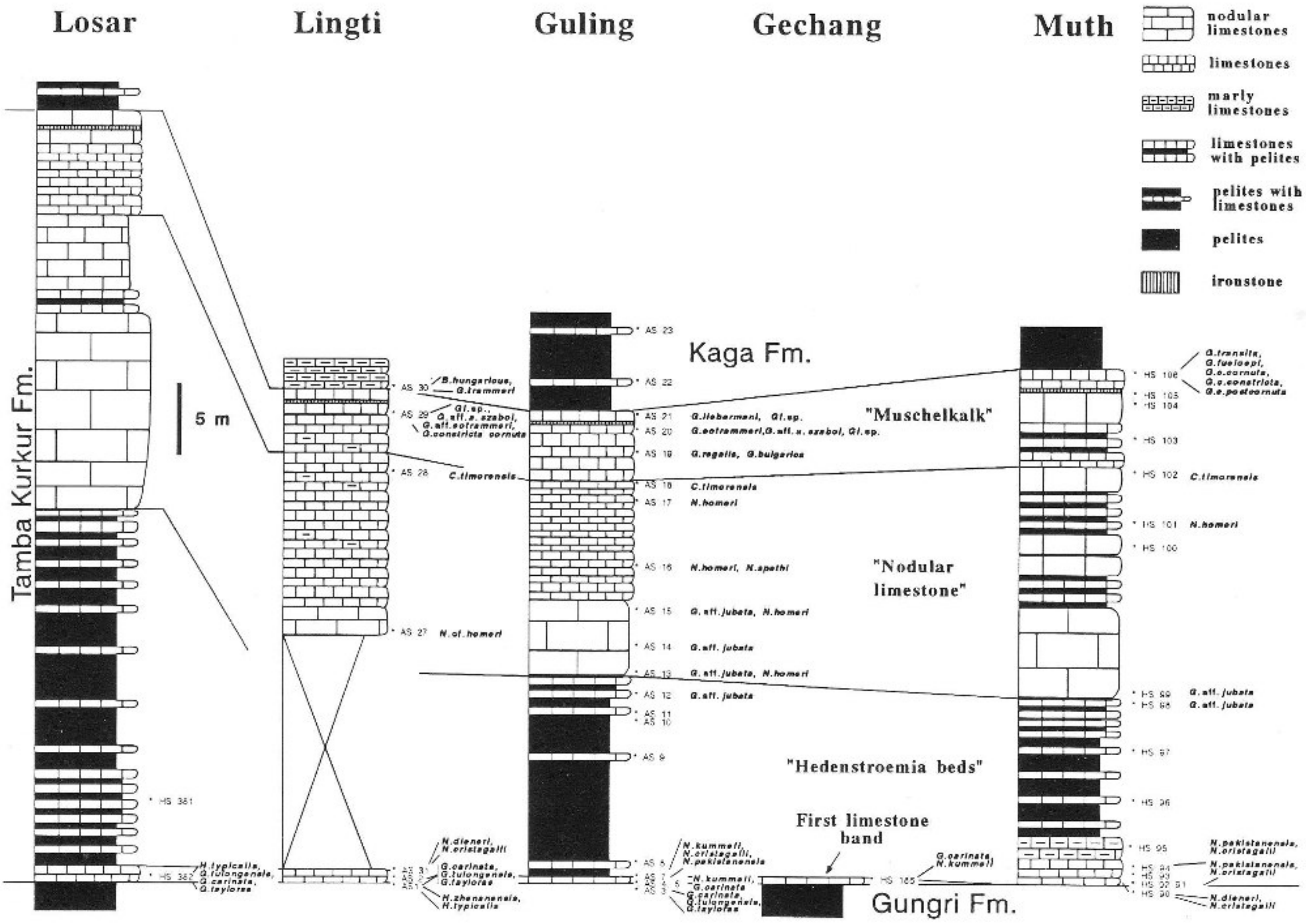

Fig. 3 - Measured stratigraphic sections in the Induan to lowermost Ladinian Tamba Kurkur Formation. Stratigraphic position of samples and conodont faunas is indicated. The Losar section was sampled for conodonts only at the base; correlation of overlying intervals is based on lithology.

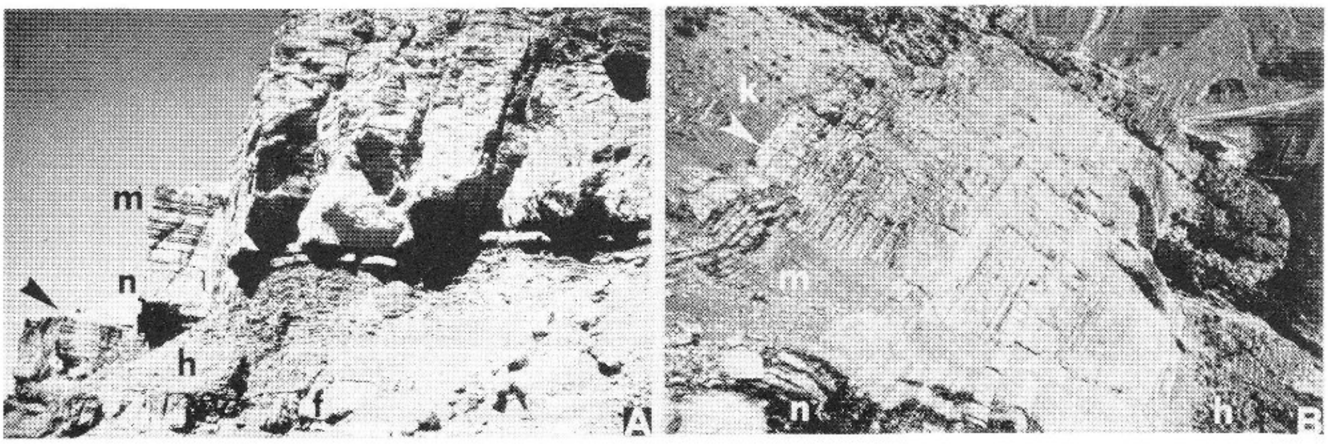

Fig. 4 - Stratigraphy of Tamba Kurkur Fm. (f= First limestone band; h= Hedenstroemia beds; n= Nodular limestone; m= Muschelkalk; k= Kaga Fm.; arrows mark sharp top of the unit). A) Above Losar (see also Fig. 5); B) at Muth.

cent Zanskar (Gaetani et al., 1986, p. 457) and Kumaon regions (Diener, 1912; Heim & Gansser, 1939).

First limestone band.

These grey-reddish, nodular, locally dolomitic, bioclastic wackestones (not represented at Muth; 0.5 m at Guling; 1.0 to 1.4 m at Lingti; 1.2 m at Losar) contain common ammonoids and conodonts (Pl. 1 and 2). The very base of the interval, containing phosphate nodules at Losar, ranges in age from Griesbachian at Losar, Lingti and Guling [(*Typicalis/Isarcica* zone: *Gondolella carinata* (Clark, 1959), *G. tulongensis* (Tian, 1982), *G. taylorae* (Orchard in Orchard, Nassichuk & Rui, 1994), *Hindeodus typicalis* (Sweet, 1970), *H. zhenanensis* (Dai & Zhang, 1989); Tab. 2] to earliest Dienerian at Gechang (base of *Kummeli/Cristagalli* zone: *G. carinata*, *Neospathodus kummeli* Sweet, 1970; Tab. 3). The top of the interval is early Late Dienerian at Lingti and Guling (base of *Pakistanensis* zone: *N. kummeli*, *N. dieneri* Sweet, 1970, *N. cristagalli* Sweet, 1970, *N. pakistanensis* Sweet, 1970; Tab. 4 and 5).

Hedenstroemia beds.

This member begins with grey bioclastic wackestones interbedded with black mudrocks (0.6 at Muth; 3.0 at Losar), yielding ammonoids and conodonts of early Late Dienerian age (*Pakistanensis* zone: *N. dieneri*, *N. cristagalli*, *N. pakistanensis*) at Muth (Tab. 6), where this interval directly overlies the Gungri Formation. Next, nodular limestones with bacterial mats and abundant ammonoids (2.9 m at Muth; 3.8 m at Losar) yielded conodonts of probably Late Dienerian age (top of *Pakistanensis* zone: *N. pakistanensis*, *N. cristagalli*, *G. nepalensis* Kozur & Mostler, 1976). An Early Smithian age is less likely, since *N. waageni* is absent. The following mudrocks, rhythmically intercalated with thin- to medium-bedded bioclastic wackestones (7.0 m at Muth; 12.6 m at Guling; 16.6 m at Losar), only locally yielded ramiform conodonts in the uppermost part. Bivalve- and crinoid-bearing packstones may occur in the middle-upper part. Next, a distinct interval of interbedded grey mudrocks and burrowed nodular mudstone/wackestones with abundant stylolites (2.6 m at Muth; 1.5 m at Guling; 1.7 m at Losar) yielded the conodont *G.* aff. *jubata* Sweet, 1970 (Garzanti et al., 1994a), suggesting a latest Smithian age (*Triangularis* zone), since *N. homeri* is absent. This is equivalent to the "Horizon of *Pseudomonotis himaica*" and "Horizon of *Rhynchonella griesbachi*" (Hayden, 1904; Diener, 1912).

Nodular limestone.

Grey-reddish amalgamated nodular wackestones with bacterial mats ("Niti Limestone" of Noetling, in Diener, 1912; 6.4 m at Muth; 5.4 m at Guling; over 2 m at Lingti; 13.8 m at Losar) yielded Spathian conodonts [*Jubata/Collinsoni* zone: *G.* aff. *jubata*, *N. homeri* (Bender, 1970)] at Guling and Muth. The overlying thick-bedded grey nodular bioclastic wackestones to packstones alternate with medium-bedded wackestones with mudrock interbeds (11.0 m at Muth; 8.4 m at Guling; 10.8 m at Lingti; 6.9 m at Losar) and yielded fish remains and conodonts. *G.* aff. *jubata*, *N. homeri* and *N. spathi* Sweet, 1970 still indicate the Spathian (*Jubata/Collinsoni* zone) up to the topmost metre, where widespread occurrence of *Chiosella timorensis* (Nogami, 1968) testifies to the earliest Aegean (*Timorensis* zone).

PLATE 1

Conodonts in Lower Griesbachian base of First limestone band of Tamba Kurkur Fm. (sample AS1, Lingti section) (sample AS3, Guling section); a) upper view; b) lower view; c) lateral view.

Fig. 1 b, c - *Hindeodus zhenanensis* (Dai & Zhang). AS1; x 65.
Fig. 2 a, b, c - *Gondolella tulongensis* (Tian). AS1; x 65.
Fig. 3 a, b, c - *Gondolella tulongensis* (Tian). AS1; x 65.
Fig. 4 a, b, c - *Gondolella taylorae* (Orchard). AS1; x 65.
Fig. 5 a, b, c - *Gondolella carinata* (Clark). AS1; x 65.
Fig. 6 a, b, c - *Gondolella taylorae* (Orchard). AS3; x 65.
Fig. 7 a, b, c - *Gondolella taylorae* (Orchard). AS3; x 65.
Fig. 8 a, b, c - *Gondolella* aff. *taylorae* (Orchard). AS3; x 65.
Fig. 9 a, b, c - *Gondolella carinata* (Clark). AS3; x 65.
Fig. 10 a, b, c - *Gondolella tulongensis* (Tian). AS3; x 65.
Fig. 11 a, b, c - *Gondolella taylorae* (Orchard). AS3; x 65.
Fig. 12 a, b, c - *Gondolella carinata* (Clark). AS3; x 65.

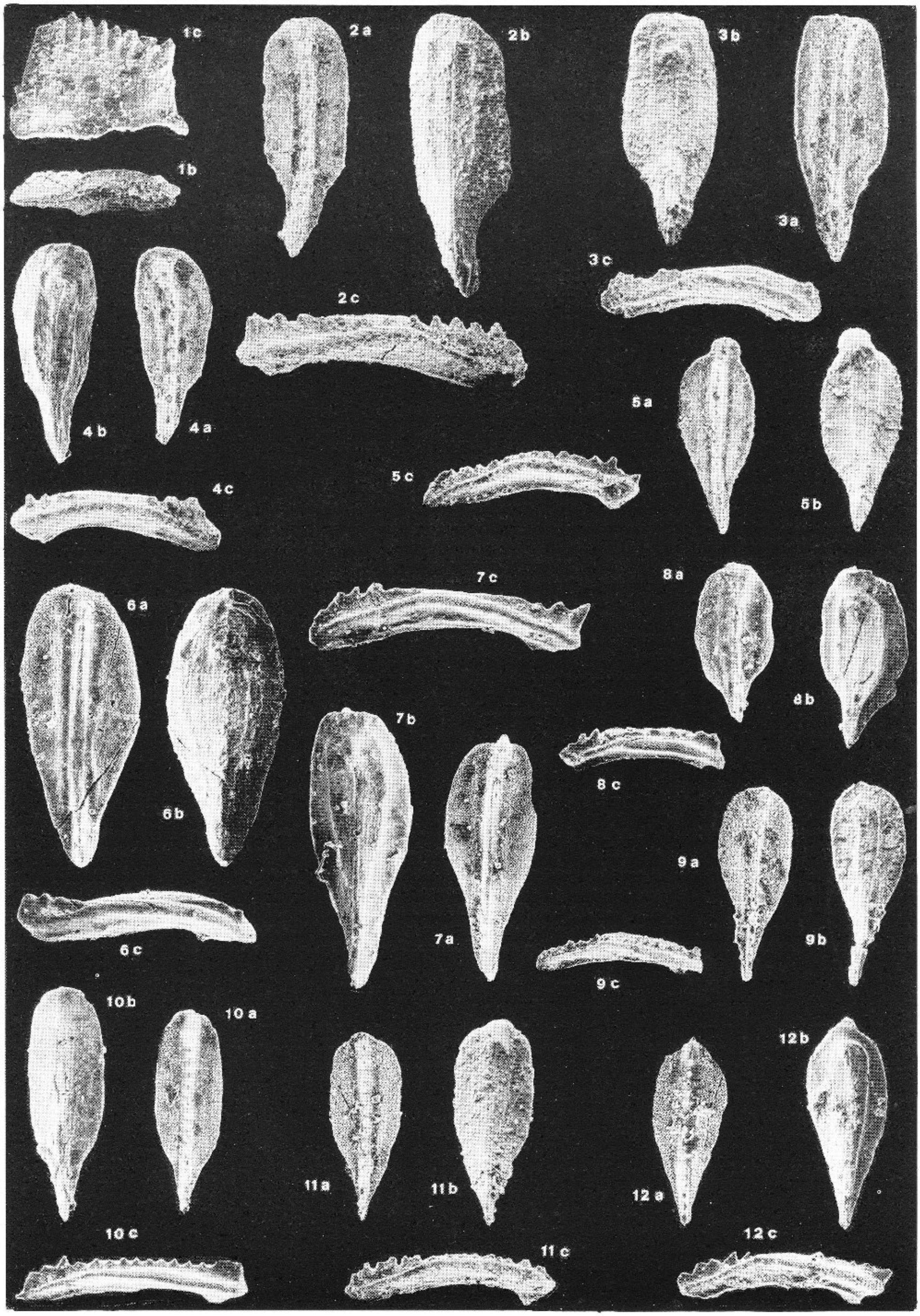
1c
1b
2a
2b
3b
3a
3c
2c
4b
4a
5a
5c
5b
4c
7c
8a
6a
8b
7b
6b
8c
9a
7a
9b
6c
9c
10b
10a
12b
11a
11b
12a
10c
12c
11c

Losar Section	metres from TK base	sample	G. tulongensis	G. taylorae	G. carinata	H. typicalis	H. sp.	Ramiforms	Zone	Age
Tamba Kurkur Fm.	6.00	HS 381			barren					
	0.00	HS 382	33	38	43	7	7	5	Typicalis/Isarcica	GRIESBACHIAN

Tab. 2 - Conodont distribution, frequency and age for base of Tamba Kurkur Fm. (TK) at Losar.

Gechang Section	metres from TK base	sample	G. tulongensis + aff. tulongensis	G. taylorae + aff. taylorae	G. carinata	N. kummeli	Ramiforms	Zone	Age
Tamba Kurkur Fm.	0,00	HS 186	3;2	3;3	37	93		Kummeli/Cristagalli	E.DIENERIAN

Tab. 3 - Conodont distribution, frequency and age for base of Tamba Kurkur Fm. (TK) at Gechang.

Lingti Section	metres from TK base	sample	H. zhenanensis	H. typicalis	G. tulongensis	G. taylorae	G. carinata	N.cristagalli	N. dieneri	N. homeri	C. timorensis	G. constricta cornuta	G. aff. eotrammeri	Gl. sp.	G. aff. a. szaboi	G. trammeri	G. foliata	B. hungaricus	Ramiforms	Zone	Age
Kaga Fm.	35,50	AS 30												1		1	7	2			LONGOBARDIAN/FASSANIAN
Tamba Kurkur Fm.	33,60	AS 29										7	1	1	1						L.ILLYRIAN
	30,80	AS 28									68								1	Timorensis	E.AEGEAN
	18,00	AS 27								2									4	Jubata / Collinsoni	SPATHIAN
	1,00	AS 31						15	6										11	Kummeli/Cristagalli	E.DIENERIAN
	0,45	AS 2			15	7	737													Typicalis/Isarcica	GRIESBACHIAN
	0,00	AS 1	1	3	33	16	815														

Tab. 4 - Conodont distribution, frequency and age for Tamba Kurkur Fm. (TK) at Lingti.

Guling Section	metres from TK base	sample	G. tulongensis + aff. tulongensis	G. taylorae + aff. taylorae	G. carinata	N. kummeli	N.cristagalli	N. pakistanensis	G aff. jubata	N. homeri	N. spathi	C. timorensis	G. regalis	G. bulgarica juvenile	G. sp. fragments	G. aff. a. szaboi	G. aff. eotrammeri	G. liebermani + G. l. transition to G.fueloepi	Gl. sp.	Ramiforms	Zone	Age
Kaga Fm.	37,67	AS 23			barren																	
	33,54	AS 22			barren																	
Tamba Kurkur Fm.	32,04	AS 21																5;3	1			
	31,29	AS 20													11	15	10			10		L.ILLYRIAN
	29,49	AS 19											214	21						30	Regalis	AEGEAN / BYTHINIAN
	28,09	AS 18										118								14	Timorensis	E.AEGEAN
	27,09	AS 17								4										19	Jubata / Collinsoni	SPATHIAN
	20,94	AS 16								7	5									24		
	18,69	AS 15							4	4										6		
	15,29	AS 14							20											2		
	13,29	AS 13							39	5										1		
	12,55	AS 12							2												Triangularis	L.SMITHIAN
	11,35	AS 11																		2	?	?
	10,45	AS 10			barren																	
	10,00	AS 9			barren																	
	1,18	AS 8			barren																	
	0,46	AS 7				7	25	8													Pakistanensis	L.DIENERIAN
	0,37	AS 6				13														2	Kummeli/Cristagalli	E.DIENERIAN
	0,32	AS 5		3	10	27														2		
	0,17	AS 4				1																
	0,00	AS 3	13;3	10;4	11															2	Typicalis/Isarcica	GRIESBACHIAN

Tab. 5 - Conodont distribution, frequency and age for Tamba Kurkur Fm. (TK) at Guling.

PLATE 2

Conodonts in First limestone band of Tamba Kurkur Fm. (sample HS382, Early Griesbachian; Losar section) (sample HS186, Early Dienerian; Gechang section) (sample AS5, Early Dienerian; Guling section); a) upper view; b) lower view; c) lateral view.

Fig. 1 a, c - *Hindeodus typicalis* Sweet. HS382; x 90.
Fig. 2 a, b, c - *Gondolella tulongensis* (Tian). HS382; x 80.
Fig. 3 a, b, c - *Gondolella taylorae* (Orchard). HS382; x 80.
Fig. 4 - *Neospathodus kummeli* Sweet. HS186; x 80.
Fig. 5 a, b, c - *Gondolella taylorae* (Orchard). HS186; x 65.
Fig. 6 - *Neospathodus kummeli* Sweet. HS186; x 80.
Fig. 7 a, b, c - *Gondolella* aff. *taylorae* (Orchard). HS186; x 80.
Fig. 8 a, b, c - *Gondolella* aff. *tulongensis* (Tian). HS186; x 65.
Fig. 9 a, b, c - *Gondolella carinata* (Clark). AS5; a) x 65; b,c) x 80.
Fig. 10 a, b, c - *Gondolella carinata* (Clark). AS5; a) x 65; b,c) x 80.
Fig. 11 - *Neospathodus kummeli* Sweet. AS5; x 80.

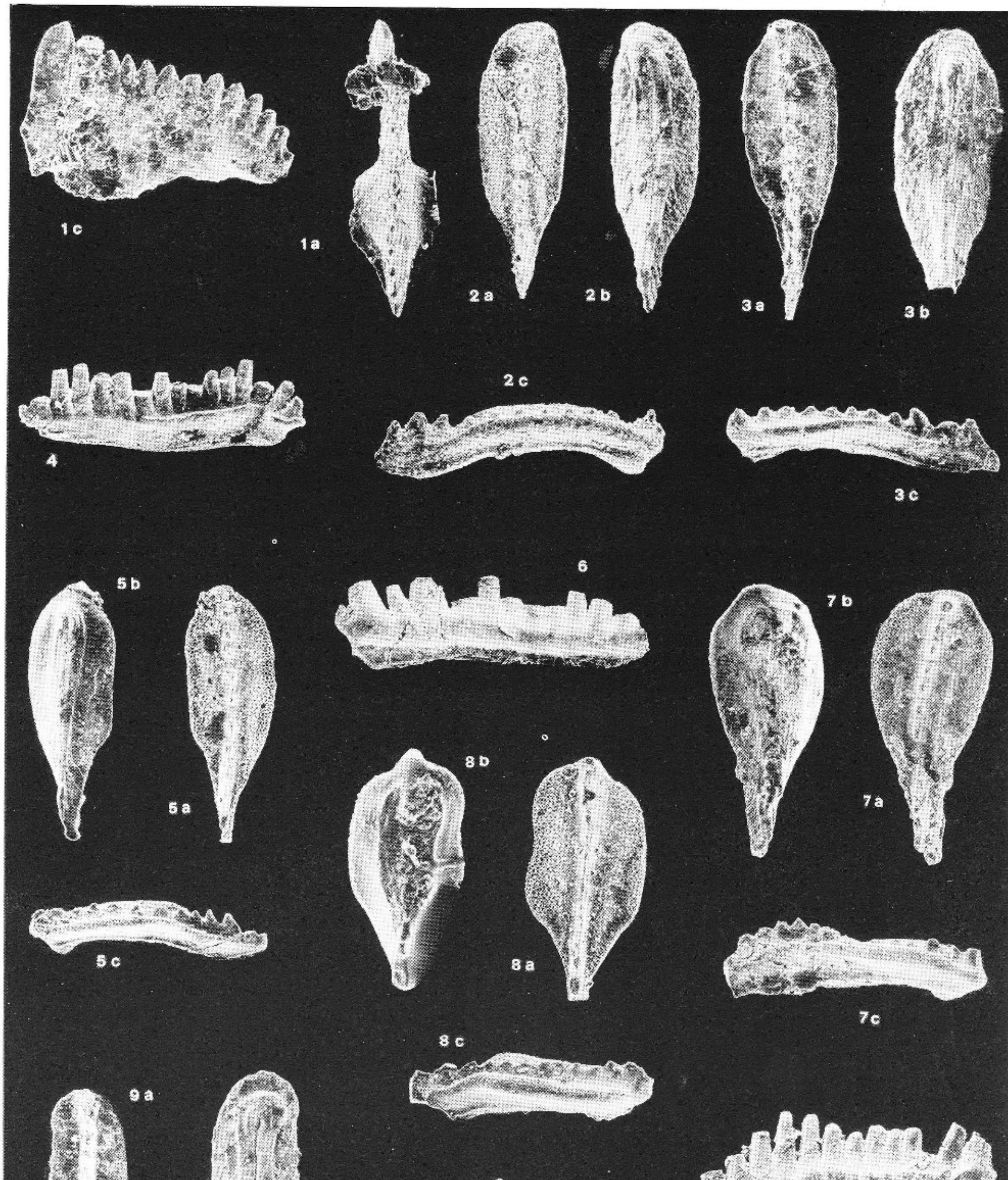
1c
1a
2a
2b
3a
3b
4
2c
3c
5b
6
7b
5a
8b
7a
5c
8a
7c
8c
9a
10b
11
9
10c
9c
10a

Muth Section	metres from TK base	sample	N. dieneri	N.cristagalli	N. pakistanensis	G. nepalensis	G aff. jubata	N. homeri	C. timorensis	G. constricta constricta	G. constricta postcornuta	G.constricta cornuta	G. fueloepi	G. transita	G. trammeri	G. sp. fragments	N. sp. fragments	Ramiforms	Zone	Age
	35,80	HS 106								2	3	3	6	3	2			15		E.LADINIAN
	34,90	HS 105		barren															?	?
	34,60	HS 104		barren																
	31,00	HS 103		barren																
	29,40	HS 102							9									1	Timorensis	E.AEGEAN
	26,20	HS 101						2										1	Jubata / Collinsoni	SPATHIAN
	24,60	HS 100		barren																
	13,00	HS 99					15									7				
Tamba Kurkur Fm.	12,20	HS 98					10									15			Triangularis	L.SMITHIAN
	10,40	HS 97		barren															?	?
	6,40	HS 96		barren																
	2,90	HS 95		22	17												35	16	Pakistanensis	L.DIENERIAN
	1,40	HS 94		20	56												>80	10		
	0,60	HS 93		8	4	4														
	0,40	HS 92		1	1															
	0,20	HS 91		78	17											49		3		
	0,00	HS 90	3	20	11													2		

Tab. 6 - Conodont distribution, frequency and age for Tamba Kurkur Fm. (TK) at Muth.

Muschelkalk.

The topmost part of the Tamba Kurkur Fm. is invariably strongly condensed (5.8 m at Muth; 4.95 m at Guling; 4.7 m at most at Lingti; 7.3 m at Losar).

The lower part (2.0 m at Muth; 3.2 m at Guling; 2.8 m at Lingti; 3.8 m at Losar) consists of medium-bedded dark-grey nodular limestones with large ammonoids and interbedded marls. The Early Bithynian is indicated by conodonts *G. regalis* (Mosher, 1970) and a few *G. bulgarica* (Budurov & Stefanov, 1975) 1.4 m above the base at Guling, whereas *G. constricta cornuta* (Budurov & Stefanov, 1972), *G.* aff. *alpina szaboi* Kovacs, 1983, *G.* aff. *eotrammeri* Krystyn, 1983 and *Gladigondolella* sp. found at the top at Lingti already document the latest Illyrian.

The upper part (3.8 m at Muth; 1.75 m at Guling; 1.9 m at Lingti; 3.5 m at Losar) consists of dark grey nodular wackestones to floatstones with abundant and locally phosphatized ammonoids or bivalves; an ostracod assemblage is reported by Pant & Azmi (1982). Latest Illyrian conodonts were found at the base at Guling (*G.* aff. *alpina szaboi, G. eotrammeri, Gladigondolella* sp.). An up to 13 cm thick glauconitic layer in the middle part yielded glauconized gastropods, ostracods, benthic foraminifers and common echinoderm plates and calcareous sponge spicules. In the upper part, corals, burrows and authigenic feldspars are observed; conodonts at Guling indicate the Anisian/Ladinian boundary (*G. liebermani* Kovacs, 1993, *G. liebermani* transitional form to *G. fuelopi* Kovacs, 1993, and *Gladigondolella* sp.; Pl. 3). The varied conodont assemblage found 50 cm below the top at Muth (*G. transita* Kozur & Mostler, 1971, *G. fueloepi* Kovacs, 1993, *G. trammeri* Kozur, 1972, *G. constricta constricta* Mosher & Clark, 1965, *G. constricta cornuta, G. constricta postcornuta* Kovacs, 1993; Tab. 6) already documents the earliest Ladinian (Nevadites Zone; Krystyn, 1983; Kovacs et al., 1990).

The condensed glauconitic layer occurring 1.1 to 1.5 m below the top of the Tamba Kurkur Formation thus roughly corresponds with the Anisian/Ladinian boundary. Moreover, the top of the Tamba Kurkur Fm. is slightly younger at Muth with respect to Guling, where a significant time gap is indicated.

Hanse Group.

The Hanse Group (333 m at Muth; about 370 m at Losar), sharply overlying the Tamba Kurkur Fm. and marking an abrupt increase in mud supply (Fig. 5), includes the largely Upper Ladinian Kaga Fm., the uppermost Ladinian to lowermost Carnian Chomule Fm., and the upper Lower to Upper Carnian "Grey beds".

Kaga Formation.

The unit (42 m at Muth; 50 to 60 m at Losar) consists predominantly of grey marls with intercalated thin to medium-bedded dark grey marly mudstones locally containing daonellids and silty marls. Crinoid- and brachiopod-bearing grey limestones and marls at the very base at Lingti yielded the conodonts *G. trammeri, G. foliata* (Budurov, 1975), juvenile *Budurovignathus hungaricus* (Kozur & Vegh, 1972) and *Gladigondolella* sp., documenting the latest Early Ladinian (latest Fassanian; Curionii Zone; Pl. 3).

PLATE 3

Conodonts at top of Tamba Kurkur Fm. (sample AS21, latest Anisian; Guling section) and at base of Kaga Fm. (sample AS30, late Early Ladinian; Lingti section); a) upper view; b) lateral view; c) lateral view.

Fig. 1 a, b, c - *Gondolella liebermani* Kovacs. AS21; a, c) x 130; b) x 120.
Fig. 2 a, b, c - *Gondolella foliata* (Budurov). AS30; x 130.
Fig. 3 a, b, c - *Gondolella trammeri* Kozur. AS30; x 130.
Fig. 4 a, b, c - *Budurovignathus hungaricus* (Kozur & Vegh). Juvenile specimen. AS30; x 130.

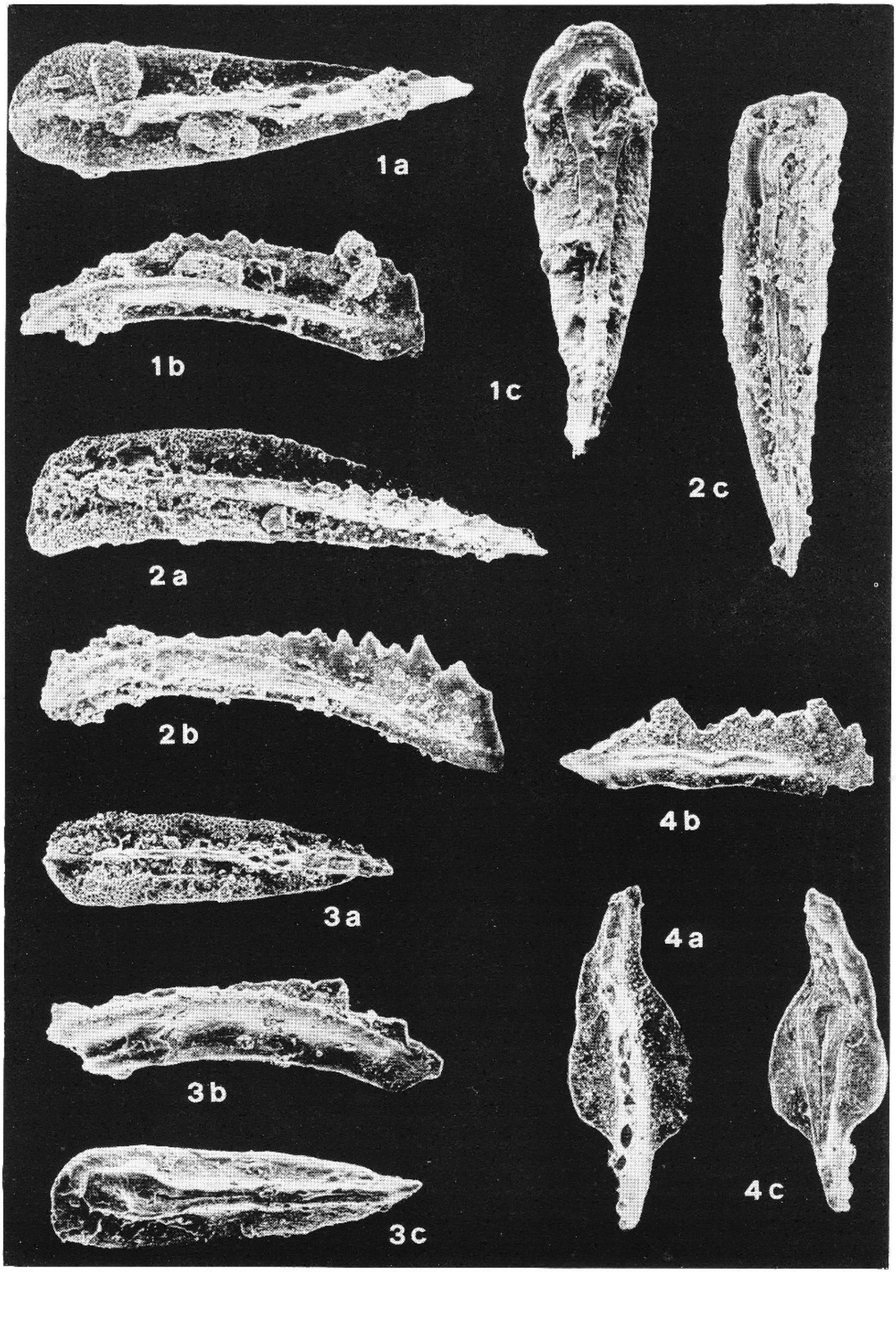
1a
1b
1c
2a
2b
2c
3a
3b
3c
4a
4b
4c

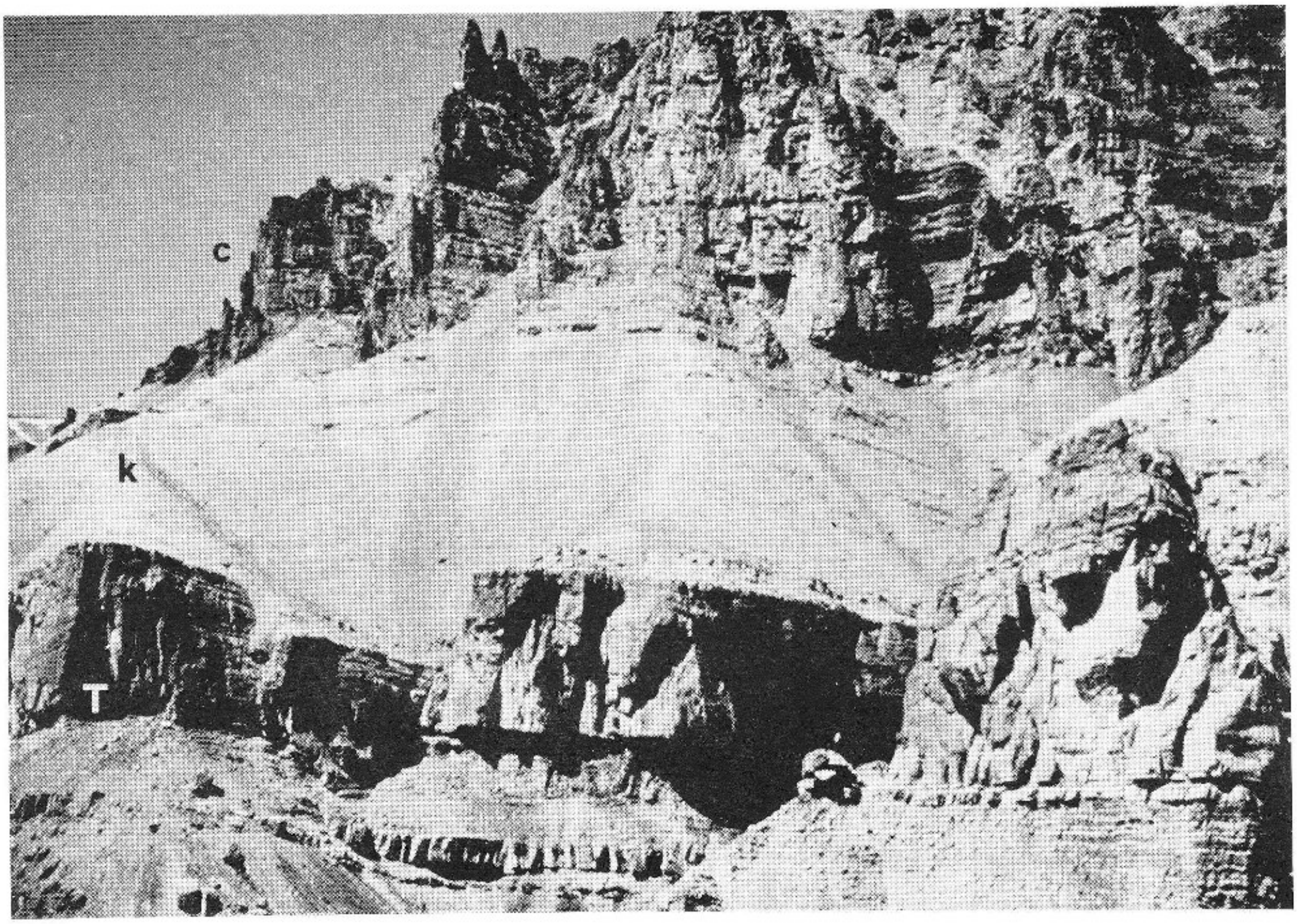

Fig. 5 - Lower-Middle Triassic succession above Losar (T= Tamba Kurkur Fm.; k= Kaga Fm.; c= Chomule Fm.).

Chomule Formation.

The unit (85 m at Muth; at least 100 m in the Gyundi river valley and more above Losar; Fig. 5) consists of dark grey medium-bedded marly mudstones and subordinate marls. Bioclastic lags are locally observed; small authigenic feldspars are very common. The lower and upper boundary are both clear-cut, and marked by rapid decrease and increase respectively of interbedded marls.

All collected samples were barren of conodonts; we are thus unable to separate an uppermost Ladinian lower part ("Daonella limestone" of Hayden, 1904) from a lowermost Carnian upper part ("Halobia limestone" of Hayden, 1904).

Grey beds.

The unit (206 m at Muth, thinner westwards) consists of interbedded marls and marly limestones, locally intensely burrowed. Phosphate nodules are rare. Mudstones in the basal 25 m are full of daonellids; higher up only a few calcarenites with thin-shelled pelecypods and ostracods or gastropods are found.

In the first metres of the unit, ammonoids and conodonts (*G. polygnathiformis* Budurov & Stefanov, 1965, *G. auriformis* Kovacs, 1977) of late Early Carnian age (Obesum/Austriacum Zone) were found (Pl. 4; Krystyn, 1983). The conodont *Metapolygnathus* sp., occurring about 80 m below the top of the unit, hints at a Late Carnian age.

Nimaloksa Formation.

The latest Carnian to Early Norian Nimaloksa Fm. (433 m at Muth; over 350 m in the Parahio valley; 450 to 500 m at Kioto), is formally subdivided into a *Lower Member*, a *Middle Member* and an *Upper Member* (the latter being equivalent to the Zozar Fm. of Zanskar; Baud et al., 1984; Jadoul et al., 1990). A similar tripartite division has been suggested by Fuchs (1982, 1987).

Lower Member.

This Member (158 m thick at Muth) begins with high-frequency shallowing-upward cyclothems (1 to 4 m-thick) made of grey marls and quartzo-feldspathic bioclastic siltstones, passing upward to silty limestones and dark grey biocalcarenites with commonly burrowed top and yielding echinoderms, brachiopods, pelecypods, foraminifers, rare bryozoans and serpulids. The base and top of cyclothems are marked locally by phosphatic nodules in marls and ferruginous impregnations in carbonates. This basal interval, 36 to 45 m-thick, marks the gradual transition from the underlying Grey beds (Fig. 6).

The overlying dark grey bio-intraclastic packstones (C1 of Fig. 7) contain echinoderms, terebratulid brachiopods, pelecypods (ostreids, *Myophoria* sp.), gastropods, small colonial corals, bryozoans, foraminifers (Fig. 9), ostracods and rare calcisponges; oncoids and coated grains occur and authigenic quartz is common. Layers of lithoclastic rudstone may occur at the base of the beds, whereas their tops may show burrows, borings and ferruginous crusts. Thin-bedded marly limestones and marls are intercalated.

The following shallowing-upward sequences (5 to 20 m thick; T1 to CT3 of Fig. 7) consist of grey marls and pelecypod-bearing siltstones with parallel- or hummocky cross-lamination, passing upward to burrowed marly mudstone/wackestones, and finally to packstone/grainstones containing ooids, intraclasts, oncoids, coated grains, pelecypods, brachiopods, crinoids, foraminifers, rare calcisponges and ammonoids.

At the top, packstone/grainstones locally display megaripples (Fig. 10C) and contain oncoids, foraminifers, crinoids, corals and ooids (C3 of Fig. 7 and 8).

The conodont *Metapolygnathus pseudoechinatus* (Kozur, 1989b) (Pl. 4), found both just above the basal transitional interval (C1 in Fig. 7) and about 50 m below the top of the Member (CT3), documents a latest Carnian age (Macrolobatus/Anatropites Zone; Orchard, 1991 a,b). Benthic foraminifers of Carnian affinity in fact occur from the base of the Member [*Astacolus carnicus* (Oberhauser), *Ophthalmidium* sp., *Tetraxis* sp., *Mesoendothyra* sp., *Endothyranella* sp., Nodosariidae, aulotortids] up to 18 m below its top [Fig. 9J; C3; *Turriglomina carnica* (Dager), *Aulotortus* ex gr. *sinuosus* Weynschenk, Trochamminidae]. Appearance of *Auloconus permodiscoides* (Oberhauser) 10 m below the top (Fig. 9L; C3) suggests that the topmost metres of the Member are Early Norian in age (R. Rettori, pers. comm., 1995).

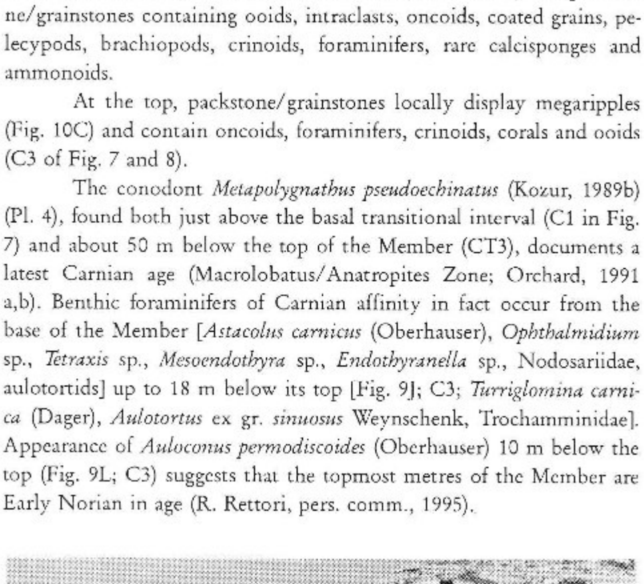

Fig. 6 - Transitional boundary between top of Hanse Group (g= Grey beds) and Nimaloksa Fm. (N) in lower Parahio valley. Note two shallowing-upward sequences capped by thick-bedded carbonates in Lower Member of Nimaloksa Fm.

Middle Member.

This Member (172 m at Muth; 205 m at Kioto) is characterized by an increase in silt-sized terrigenous detritus from the Pin and Parahio valleys to the Kioto area. Two lithozones were distinguished.

The *lower lithozone* (T2 to T4 of Fig. 7) consists of shallowing-upward sequences, thicker in the upper part and beginning with up to very fine-grained hybrid quartzo-feldspathic arenites, displaying scoured base and mudclasts or parallel- to hummocky cross-lamination and current ripples (NE-ward to SE-ward paleocurrents). Rare disarticulated megalodontids and *Rhizocorallium*- to *Zoophycos*-type burrows occur. Sequences are completed by bio-intraclastic packstone/grainstones containing oncoids, coated grains, commonly micritized radial-fibrous ooids (Fig. 9H), pelecypods, echinoderms, rhynchonellid brachiopods, small and encrusting foraminifers [*Aulotortus* ex gr. *communis* (Kristan), *Planinvolutina* sp., *Tolypammina* sp.; Fig. 9G], bryozoans (*Tebitopora* sp.; Fig. 9I). The top of the sequences is commonly marked by minor unconformities with *Skolithos*-type burrows (Fig. 10B) and layers of lithoclastic rudstone.

The *upper lithozone* (CT5 to CT10 of Fig. 7) displays an overall shallowing-upward trend, beginning with bioturbated or parallel-laminated dark grey siltstones and silty marls with small phosphatic nodules and mudclasts. Next, siltstone/carbonate cyclothems displaying hummocky cross-lamination or burrowed (Fig. 10D; 2 to 12 m thick) are followed by oncoidal packstone/rudstones with ooids, echinoderms, pelecypods and benthic (lagenids) or encrusting foraminifers (Fig. 9E). At the top, bioturbated ooidal packstone/grainstones, still intercalated with marly wackestones and silty interbeds, contain corals (most common at Muth; Fig. 9F), bryozoans, brachiopods, benthic foraminifers (Duostominidae, *Mesoendothyra* sp.), a few dasycladacean algae, calcisponges and problematica (*Baccanella* sp.). Cross-lamination (Fig. 10A) or lenses of lithoclastic rudstone are observed. Gypsum pseudomorphs and authigenic quartz or Fe-rich dolomite are widespread.

The conodont *Metapolygnathus primitius* (Mosher, 1970), found 23 m below the top at Muth (Pl. 4; CT10) documents an earliest Norian age (Kerri/Jandianus Zone; Kovacs & Kozur, 1980; Krystyn, 1980; Orchard, 1991a,b).

Upper Member.

This Member (103 m at Muth; 100 to 110 m in the Parahio valley; 158 m at Kioto) is made of shallow-water carbonates. Grey lenticular oolitic bars and thick-bedded, cross-laminated biocalcarenites with oncoids, ooids, bryozoans, brachiopods, pass upward to cross-laminated intra-bioclastic packstone/grainstones (SE-ward paleocurrents); graded lithoclastic rudstone/floatstones are intercalated. A marker horizon of stromatolitic dolostones in 50 to 70 cm-thick beds (C7 in Fig. 7 and 8) may include thin loferitic breccias, intraclastic foraminiferal packstone/grainstones (Fig. 9D) or megalodontid-bearing limestones.

Intra-bioclastic wackestone/packstones with ooids, foraminifers, echinoderms, ostracods or bryozoans and calcisponges (Fig. 9C) are common in the Parahio valley; even more distal lithofacies are arranged in four thickening-upward sequences of upward decreasing thickness in the Kioto section.

In the middle part of the Member, cross-laminated oolitic and oncoidal grainstones (Fig. 10E) to bio-oo-intraclastic packstone/rudstones yielded encrusting foraminifers, dasycladacean algae, corals (*Montlivaltia* sp.), calcisponges and rare megalodontids.

The upper part includes marly limestones and marls (CT11 in Fig. 7 and 8), bio-oo-intraclastic grainstones with oncoids, micritized ooids, echinoderms, brachiopods, foraminifers or bryozoans (Fig. 9A,B) and wackestone/packstones with pelecypods, gastropods or corals.

The top of the Member is marked by a major disconformity in the Spiti valley. Above Hal village (Fuchs, 1982, p. 347), wackestone/packstones followed by mudstones with foraminifers and authigenic bipyramidal quartz are extensively burrowed and bored (Fig. 12I). Sedimentary dykes, filled with hybrid sand derived from the overlying unit, carbonate lithoclasts and authigenic Fe-dolomite, penetrate down to 1.3 m below the top of the Nimaloksa Formation; their side-walls display ferruginous haloes and are locally encrusted by phosphate. At Kioto, the unit is capped by an intensely burrowed, peloid-bearing packstone, containing geodes filled by dolomite. A low-angle uncon-

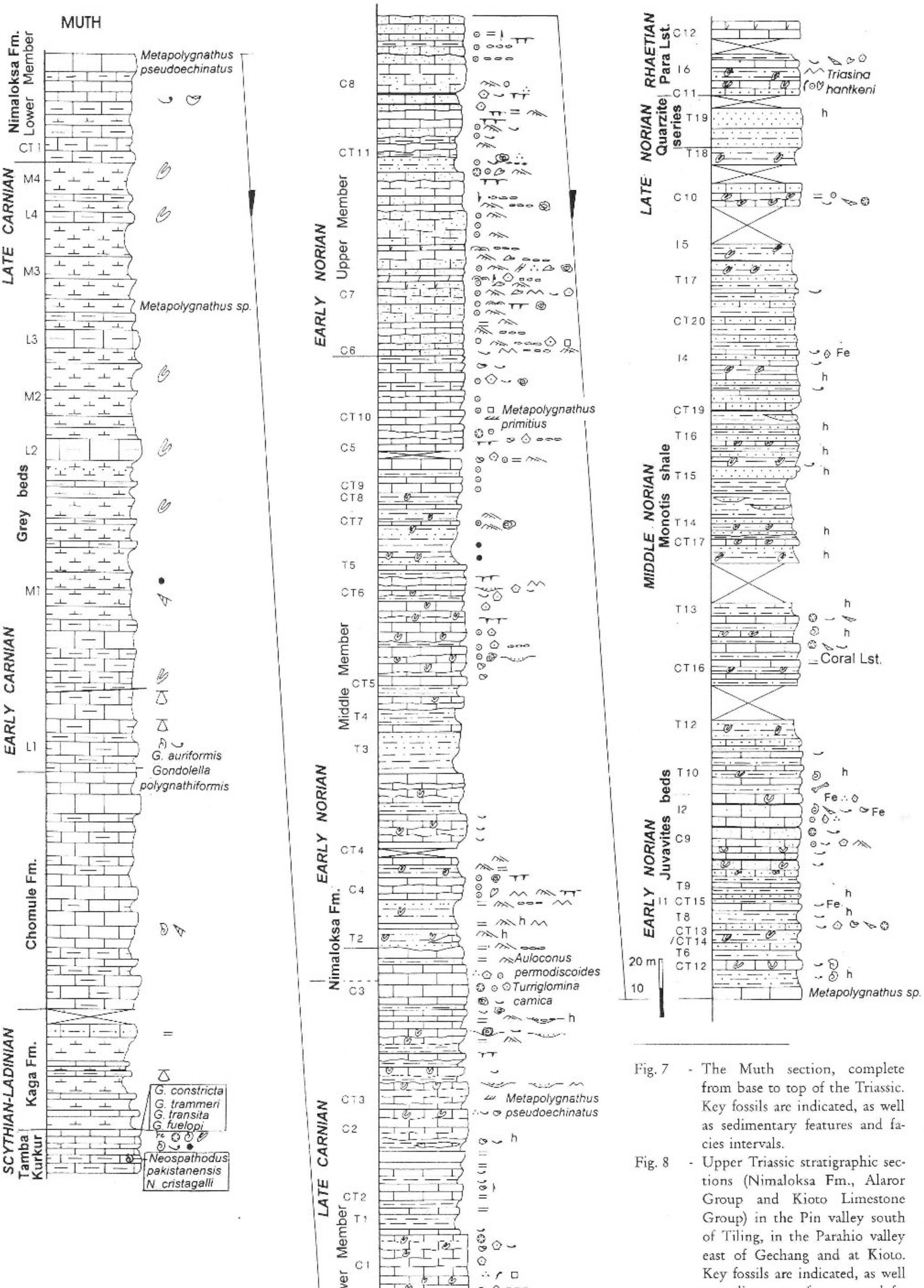

Fig. 7

Fig. 7 - The Muth section, complete from base to top of the Triassic. Key fossils are indicated, as well as sedimentary features and facies intervals.

Fig. 8 - Upper Triassic stratigraphic sections (Nimaloksa Fm., Alaror Group and Kioto Limestone Group) in the Pin valley south of Tiling, in the Parahio valley east of Gechang and at Kioto. Key fossils are indicated, as well as sedimentary features and facies intervals.


TILING
PARAHIO
KIOTO
RHAETIAN Para Lst.
LATE NORIAN
MIDDLE NORIAN Monotis shale
Coral Lst.
Juvavites beds
EARLY NORIAN
Nimaloksa Fm.
Upper Member
Middle Member
Lower Member
LATE CARNIAN
Quarzite series
Cyrtopleurites sp.
Epigondolella abneptis
30 m
10
20 m
sandstone
hybrid arenite
siltstone
marl
marly limestone
calcarenite
micritic limestone
dolomitic limestone
paraconglomerate
ooid
hummocky lamination
parallel lamination
normal/reverse graded-bedding
cross-lamination
ripple
mudclast
intraclast
bioturbation
bored surface/ unconformity
slumping
erosional surface
tepee
stromatolite
fenestrae
Fe Fe-rich layer
phosphate nodule
vertebrate bone
pelecypod
pelagic pelecypod
megalodontid
gastropod
bryozoan
foraminifer
ammonoid
brachiopod
coral
crinoid/echinoid
oncolite
conodont
F fault
Sedimentary events
M marly facies
L marly limestone facies
C carbonate facies
T terrigenous facies
CT carbonate/terrigenous facies
I ironstone/phosphatic facies

Fig. 8

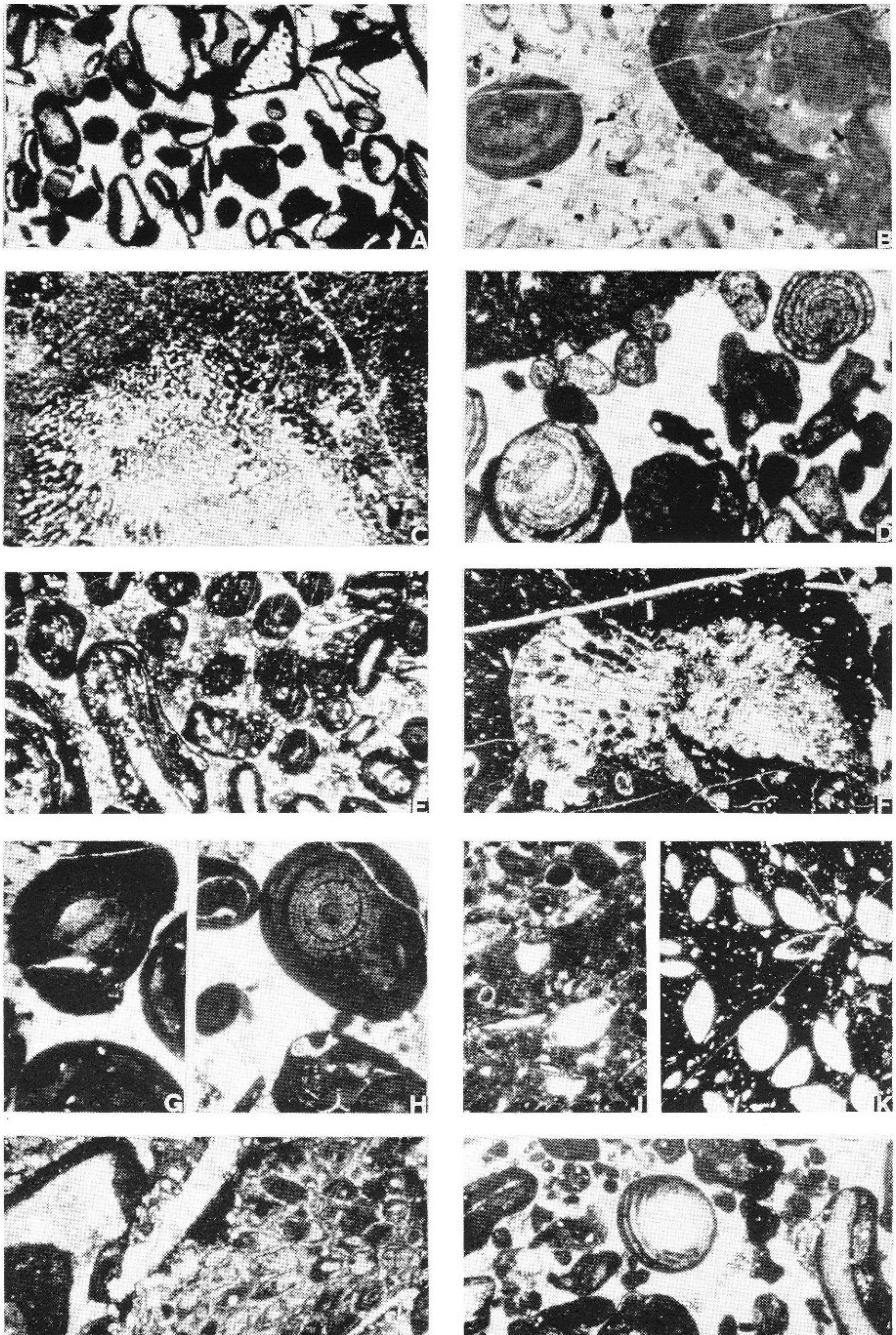
A
B
C
D
E
F
G
H
J
K
I
L

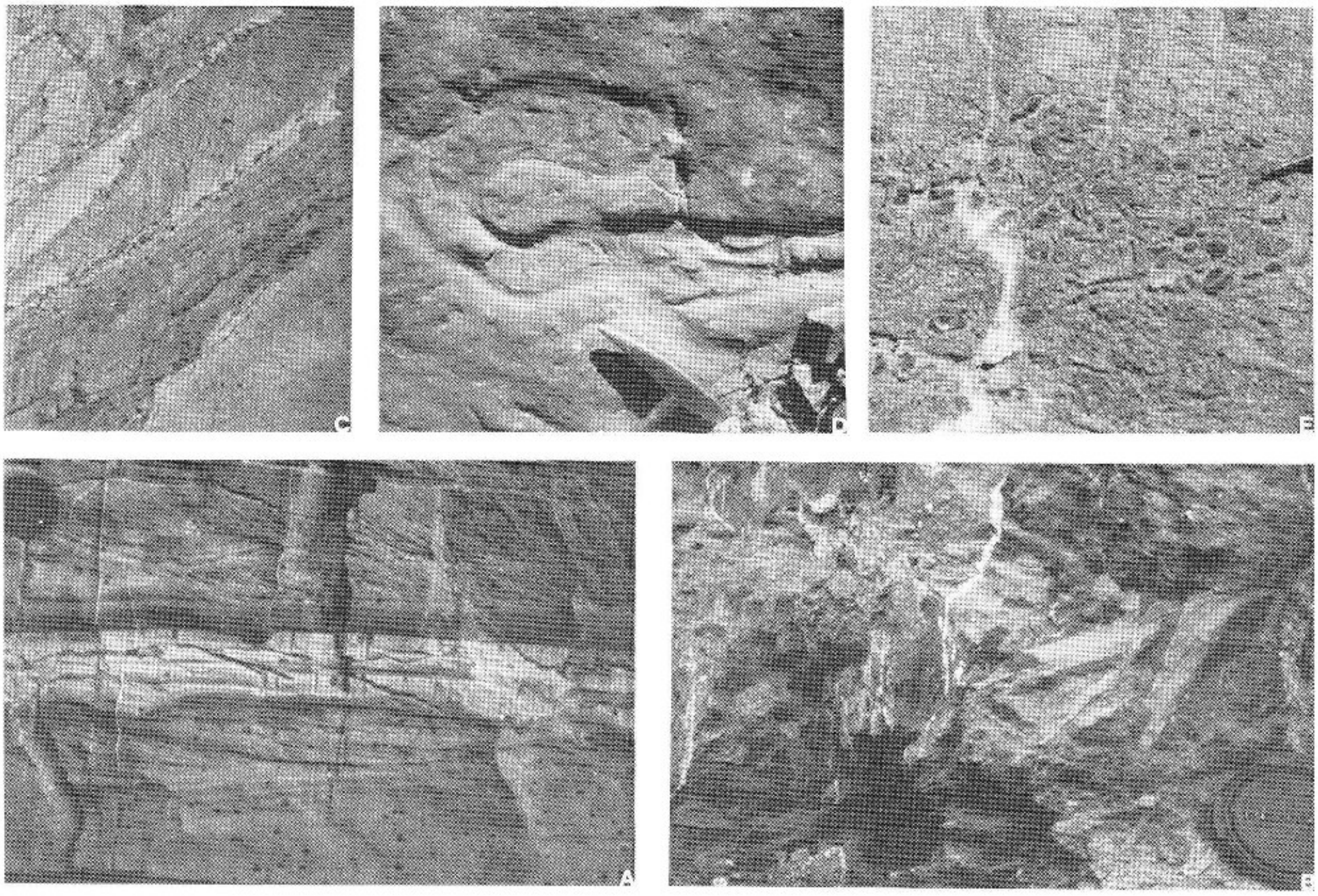

Fig. 10 - Sedimentary features of Nimaloksa Formation. A) Hummocky (below) to ripple and megaripple cross-lamination in hybrid intraclastic calcarenites with intercalated mudstone (Middle Member; Parahio valley). B) Subvertical burrows in wackestone/packstone at top of high-frequency cyclothem (Middle Member; Parahio valley). C) Small megaripples (amplitude 20 cm) on bedding surfaces of intraclastic packstones (Lower Member; Muth). D) Large *Rhizocorallium*-type burrow in silty limestone at base of high-frequency cyclothem (Middle Member; Muth). E) Oncoidal packstone/rudstone with bioclasts, ooids and intraclasts, scoured by hybrid arenite (Upper Member; Muth).

formity can be recognized also in the Parahio valley and Muth (Fig. 13A,B), where ammonoids and *Zoophycos*-type burrows are observed on the top of the Nimaloksa Fm.; hardgrounds marked by up to 40 cm-deep vertical burrows may be filled with ochre-reddish sediment.

Foraminiferal assemblages (*Aulotortus friedli* Kristan-Tollman, *A.* ex gr. *sinuosus*, *A.* ex gr. *communis*, *Glomospira* sp., *Mesoendothyra* sp., Textulariidae, Variostomatidae, Nodosariidae) indicate a Norian age (R. Rettori, pers. comm., 1995).

Alaror Group.

The Alaror Group (321 m at Muth; 353 m at Kioto), unconformably overlying the Nimaloksa Fm. and late Early Norian to mid-Rhaetian in age, is traditionally subdivided into four units (Fig. 11; "*Juvavites* beds", "Coral limestone", "*Monotis* shale" and "Quartzite series" in ascending order; Hayden, 1904; Diener, 1908; Fuchs, 1982). These classical lithostratigraphic subdivisions, displaying an overall sandier-upward trend punctuated by the coral-bearing carbonate band in the middle, have been given formational status (i.e., Bhargava, 1987) even though they are difficult to trace laterally, due to poor original definition and strong lateral variability of facies (more common sandstones and grainstones at Muth, predominating siltstones and mudstones at Kioto).

Fig. 9 - Microfacies of Nimaloksa Formation. A) Bio-intraclastic grainstone with coated grains and *Aulotortus*–ex gr. *communis* (C8: top of Upper Member, Muth; x 25 JS 150). B) Oncoidal rudstone with composite oncoids and small forams (?*Glomospira* sp.; Endothyridae) (CT11: Upper Member, Muth; x 25 JS 149). C) Intraclastic packstone with ?calcisponge (C7: Upper Member, Muth; x 11 JS 147). D) Bio-intraclastic grainstone with aulotortids (C7: Upper Member, Muth; x 25 JS 146). E) Oncoidal packstone/rudstone; note borings in pelecypod at oncoid core (CT7: Middle Member, Muth; x 11 JS 139). F) Floatstone with corals (C5: Middle Member, Parahio; x 11 JS 20). G, H) Oncoidal grainstone with *Aulotortus* ex gr. *communis* and radial-fibrous ooids at oncoid core (C4: Middle Member, Muth; x 25 JS 132). I) Rudstone with bryozoans (*Tebitopora* sp.), coated bioclasts and quartzose silt (T2: Middle Member, Parahio; x 25 JS 5). J) Bio-intraclastic packstone with *Aulotortus* ex gr. *sinuosus* (C3: Lower Member, Muth; x 25 JS 128). K) Wackestone/packstone with recrystallized aulotortids (C1: Lower Member, Muth; x 11 JS 122). L) Oncoidal bio-intraclastic grainstone with *Auloconus permodiscoides* (C3: Lower Member, Muth; x 25 JS 129).

Further observations are thus needed before the informal but long- and widely-known terminology could be usefully replaced by new formal names. The terms Hangrang and Nunuluka Fms. (equivalent to "Coral limestone" and "Quartzite series" respectively; Bhargava, 1987) were not adopted in the studied localities, where the true "Coral limestone" (knoll reefs of limited areal extent; Bhargava & Bassi, 1985) is not present, and the upper transitional boundary between the "*Monotis* shale" and the "Quartzite series" could be only somewhat subjectively established.

Juvavites beds.

The *Juvavites* beds (109 m at Muth; 197 m at Kioto) can in turn be subdivided into three lithozones: the lower and upper ones consist of muddy terrigenous to calcareous shelf sediments, whereas grainstones and oolitic ironstones characterize the middle one.

Thickness of the *lower lithozone* markedly increases from 23 m at Muth to 40 m in the Parahio valley to 76 m at Kioto. In the Kioto area, its base (0.95 m at Hal; 0.2 m at Kioto), displaying particularly strong erosion at Hal, is represented by lithoclastic rudstones containing flat mudstone clasts with ferruginous rims (up to 25 cm in size), scoured from the underlying Nimaloksa Formation (Fig. 16). Abundant bioclasts (echinoderms, pelecypods, nodosariid foraminifers, brachiopods, ostracods, bryozoans), ooids, grapestones, coated grains, peloids and variable amounts of detrital quartz occur. Similar sediments fill in the dykes which penetrate well below the top of the Nimaloksa Formation. Next, hybrid arenites with hummocky cross-lamination and locally still containing small lithoclasts at the base, grey silty limestones and micaceous siltstones (6.0 m at Muth; 1.35 at Hal; 3.0 m at Kioto), are followed by burrowed mudstones to packstones containing at the base ammonoids and conodonts (*Metapolygnathus* sp.) and interbedded with siltstones and marls in the upper part (16.7 m at Muth; 9.2 m at Hal; 73 m at Kioto). In the Parahio valley, siltstones with *Zoophycos*-type burrows are intercalated with marly limestones.

The *middle lithozone* (45 m at Muth; about 60 in the Parahio valley; 34 m at Kioto; 30 m or more at Hal) consists of ferruginous hybrid arenites and calcareous to micaceous subarkosic siltstones displaying hummocky cross-lamination or burrowed, interbedded with bioclastic packstone/grainstones displaying mainly NW-ward herringbone cross-lamination at Muth. Bioclasts, commonly concentrated in storm lags and locally showing microborings, include pelecypods, crinoids, brachiopods, corals, gastropods, ostracods, algae. Very unusual, spherical to elliptical and deformed tangential ooids characterized by cross extinction with crossed nicols, typically occur in these layers. The 11 m-thick ironstone capping the lithozone at Muth (I2; Fig. 7 and 13C) is made of oolitic and bioclastic grainstones yielding echinoderms, foraminifers (*Aulotortus* ex gr. *sinuosus*, Nodosariidae) bryozoans, gastropods, pelecypods, ammonoids, ostracods. Cores of ooids, which show different stages of evolution and are commonly aggregated in lumps, commonly consist of echinoderm or foraminifer remains (Fig. 12H). Most grains are blackened and hematitized, and black goethitic ooids are widespread (Fig. 12F,G); chamositic ooids and chamosite are subordinate. Quartzose silt is minor. Hybrid siltstones and arenites with hummocky cross-lamination are capped by ferruginous intra-bio-oo calcarenites locally with lithoclasts and megalodontids in the Parahio valley, and by bioclastic packstones with tangential ooids displaying pseudo-uniaxial cross and phosphates at Kioto (Fig. 12E).

The *upper lithozone* (41 m at Muth; 87 m at Kioto) consists of cyclically interbedded orange-weathering silty limestones, locally showing hummocky cross-lamination or thin-shelled pelecypods, and burrowed dark grey siltstones with rare phosphate nodules; shales become predominant upward. Locally abundant vertebrate ribs (probably of ichthyosaurs; Fig. 13D) and rare phosphatized ammonoids characterize the base at Muth. In the Parahio and Kioto areas, silty limestones are replaced by marly siltstones locally with ammonoids.

A largely late Early Norian age (Magnus Zone) is suggested (Diener, 1908).

Coral limestone.

The Coral limestone (16 m at Muth; about 20 m in the Parahio valley; 22 m at Kioto) is a discontinuous marker lithozone (CT16 in Fig. 7 and 8) of grey nodular bioclastic limestones, with interbedded burrowed ferruginous siltstones containing phosphate nodules and very fine-grained arkoses. Hybrid biocalcarenites at Muth contain echinoderms, coral fragments, pelecypods, brachiopods and sparse bryozoans, gastropods, foraminifers and ammonoids (Fig. 13E); erosional lithoclastic lenses also occur. A similar interval of nodular limestone and biocalcarenites at Tiling yielded the conodont *Epigondolella abneptis abneptis* (Huckriede, 1958), indicating an Early/Middle Norian age (Krystyn, 1980). Packstone/grainstones with silicified bioclasts, calcisponges (*Colospongia* sp.), peloids and black grains characterize the Parahio valley section. At Kioto, siltstones displaying hummocky cross-lamination and climbing ripples (laminae dipping NE-ward to SW-ward) are intercalated with nodular mudstone/wackestones. In the studied sections patch reefs are absent; coral colonies were observed only in the scree at Lingti.

Monotis shale.

The *Monotis* shale (162 m at Muth; about 118 m at Kioto) also may be subdivided into three lithozones: shelf mudrocks with intercalated NCI-bearing hybrid arenites prevail in the lower and upper ones, whereas the middle one largely consists of storm sandstones.

PLATE 4

Conodonts at base of Grey beds (sample HS 157, late Early Carnian) and in Lower (samples JS119 and JS 125, latest Carnian) to Middle Member (sample JS 142, earliest Norian) of Nimaloksa Fm. (Muth section); a) upper view; b) lateral view; c) lateral view.

Fig. 1 a, b, c - *Gondolella polygnathiformis* Budurov & Stefanov. HS157; x 80.
Fig. 2 a, b, c - *Gondolella polygnathiformis* Budurov & Stefanov. HS157; x 80.
Fig. 3 a, b, c - *Gondolella auriformis* Kovacs. Juvenile growth stage. HS157; x 100.
Fig. 4 a, b, c - *Metapolygnathus pseudoechinatus* (Kozur). Broken specimen at the anterior end. JS119; x 80.
Fig. 5 a, b, c - *Metapolygnathus pseudoechinatus* (Kozur). Broken specimen at the anterior end. JS119; x 80.
Fig. 6 a, b, c - *Metapolygnathus* cf. *pseudoechinatus* (Kozur). Broken specimen. JS125; x 100.
Fig. 7 a, b, c - *Metapolygnathus primitius* (Mosher). JS142; x 90.

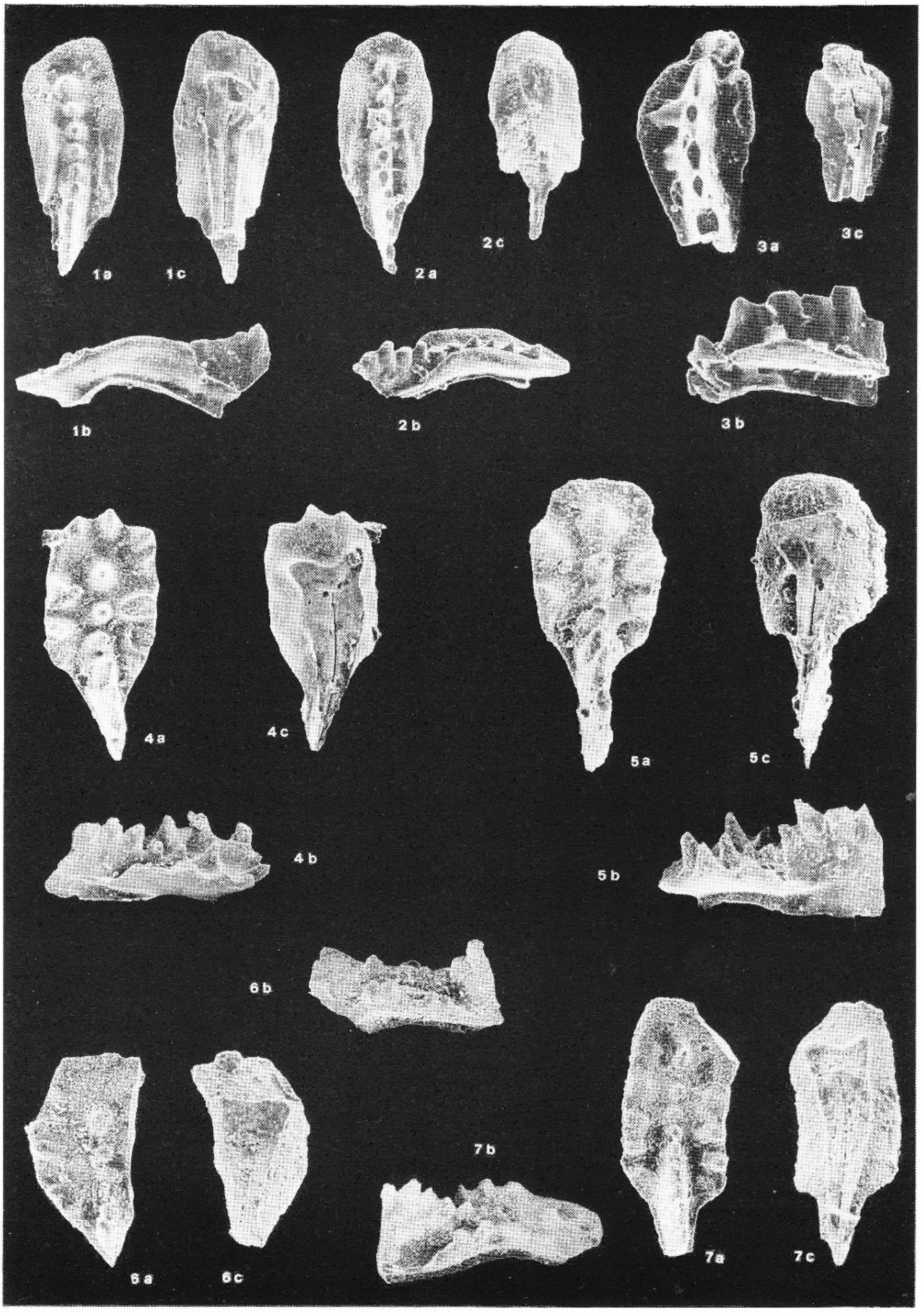
1a
1c
2a
2c
3a
3c
1b
2b
3b
4a
4c
5a
5c
4b
5b
6b
7b
6a
6c
7a
7c

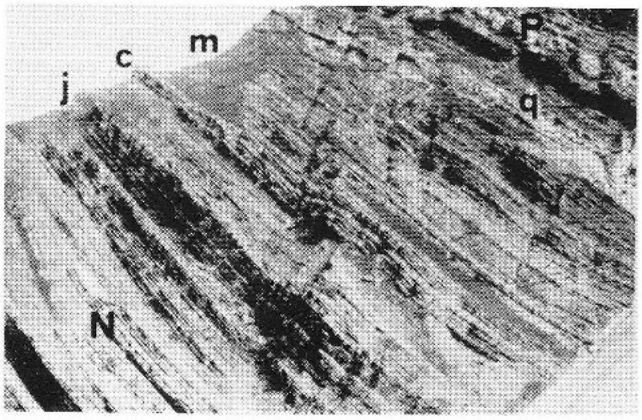

Fig. 11 - Alaror Group at Muth (N= top of Nimaloksa Fm.; j= *Juvavites* beds; c= Coral limestone; m= *Monotis* shale; q= Quartzite series; P= Para Limestone).

The *lower lithozone* (49 m at Muth; about 46 m at Kioto) begins with predominant burrowed siltstones (18.3 m at Muth; about 22 m at Kioto). The base of the lithozone, still containing corals and crinoids at Muth, at Tiling yielded ammonoids (*Cyrtopleurites* sp.; determination by M.Balini, 1995) of early Middle Norian age (Rutherfordi/Bicrenatus Zone), associated with brachiopods and phosphate nodules. Next, sharp based, very fine-grained grey calcareous arkoses displaying hummocky cross-lamination and silty limestones (9.5 m at Muth; 8.2 m at Kioto, where mudstones predominate) pass upward to prevailing burrowed siltstones with intercalated very fine-grained, grey, calcareous arkoses displaying hummocky cross-lamination or current ripples (21.4 m at Muth; 16 m at Kioto, where marly mudstones are common).

In the *middle lithozone* (20.7 m at Muth; 18 m at Kioto), coarse siltstones to very fine-grained greenish arkoses displaying parallel- to hummocky cross-lamination, climbing ripples, prod marks and "ball & pillow" structures predominate over burrowed mudrocks. Current ripples suggest multidirectional paleocurrents. Bioclastic lags and hybrid arenites contain echinoderms, bivalves, rare foraminifers (aulotortids), lithoclasts and black grains.

The *upper lithozone* (92 m at Muth; about 54 m at Kioto, where faulting occurs) begins with bivalve-bearing calcarenites, interbedded with very fine-grained greenish arkoses showing hummocky cross-lamination, burrowed siltstones and black shales (27.7 m at Muth; over 10 m at Kioto). Graded to parallel- and hummocky cross-laminated calcarenite/calcirudites show scoured bases and contain bioclasts (echinoderms, brachiopods, pelecypods, foraminifers including *Aulotortus* ex gr. *sinuosus*, calcisponges, porostromate algae), lithoclasts and peloids; microborings are common. Chamosite, black grains and silicate peloids occur at the top at Muth, in ferruginous biocalcarenites with basal lithoclastic lag and displaying hummocky cross-lamination or long burrows on stratal surfaces (Fig. 12B,C).

Next, siltstones locally with phosphate nodules interbedded with bivalve-bearing biocalcarenites (30.3 m at Muth; over 20 m at Kioto) are capped at Muth by greenish hybrid arkoses to quartz-rich subarkoses containing echinoderms, bivalves, foraminifers, greenish to black chamosite-goethite ooids (Fig. 12D), yellow-green chamositic intraclasts and shark teeth (I5 in Fig. 7; 6.5 m). At the top of the lithozone (27.8 m at Muth; 20 m at Kioto), poorly-exposed burrowed siltstones alternate with grey marly to arenaceous limestones and biocalcarenites, locally showing scoured bases and containing rounded or microbored bioclasts (pelecypods, echinoderms, brachiopods, gastropods, corals) and lithoclasts. Hybrid limestones containing streaks and lenses of bioclastic quartzarenites showing ripple or even W-dipping megaripple cross-lamination characterize the Muth section, whereas burrowed marly mudstones to wackestone/packstones and interbedded calcareous sandstones displaying hummocky cross-lamination prevail at Kioto.

Quartzite series.

The Quartzite series (34 m at Muth; 16 m at Kioto) consists of very fine- to lower fine-grained grey arkoses, upper fine-grained subarkoses and medium-grained greenish to pinkish quartzarenites, with intercalated burrowed siltstones, hybrid arenites and biocalcarenites commonly yielding pelecypods, echinoderms, foraminifers (mainly aulotortids) and gastropods (T19 in Fig. 7). Megalodons are also found locally. Scoured bases, hummocky cross-lamination and ripples, or megaripple and herringbone cross-lamination (NW-ward to SE-ward paleocurrents) are observed; dolomitic to phosphatic clasts and peloids occur.

The upper boundary is marked by sharply decreasing frequency of quartzose sandstones (Fig. 14A,B).

Para Limestone.

The base of the Kioto Group (22 m in the Muth area; 20 m at Kioto) is sharp and marked by widespread occurrence of large megalodontids (C11; Fig. 7 and 14C). Quartzose packstone/grainstones with ooids, coated grains, lithoclasts, bivalves, echinoderms and foraminifers (Fig. 12A), interbedded with burrowed grey marly mudstones and siltstones, are followed by locally dolomitized burrowed mudstones to cross-laminated blue-grey packstones with megalodons and alatochonchids.

Foraminiferal assemblages (*Triasina hantkeni* Majzon, *T. oberhauseri* Koehn-Zaninetti & Brönnimann, *Aulotortus* ex gr. *communis*, *Nodosaria* sp.) point to a Rhaetian age for the base of the unit.

The overlying interval (18 m in the Muth area; at least 18 m at Kioto, where the upper part is faulted) still includes very fine-grained arkoses to feldspathic quartza-

Fig. 12 - Microfacies of Alaror Group and base of Kioto Group. A) Recrystallized packstone/grainstone with coated bioclasts and ooids; note *Aulotortus* ex gr. *communis* at ooid core, along with *Nodosaria* sp. and crinoids (C11: Para Limestone, Tiling; x 25 JS 155). B) Bioclastic grainstone/rudstone with porostromate algae, pelecypods and iron-stained bioclasts (I4: *Monotis* shale, Muth; x 25 HS 139). C) Lithoclastic grainstone with ooids, bored *Aulotortus* ex gr. *sinuosus*, gastropods and other iron-stained bioclasts (I4: *Monotis* shale, Muth; x 25 HS 139). D) Hybrid subarkose with chamosite-goethite ooids (I5: *Monotis* shale, Muth; x 25 HS 140. E) Oo-bioclastic grainstone/rudstone with bored pelecypods, echinoids, coated grains and recrystallized tangential ooids (I2: *Juvavites* beds, Kioto; x 11 HS 354). F, G) Grainstone with goethitic ooids and blackened bioclasts (*Aulotortus* ex gr. *sinuosus*, echinoderms) (I2: middle *Juvavites* beds, Muth; x 60 HS 120-119). H) Grainstone with blackened ooids and bioclasts (*Aulotortus* ex gr. *sinuosus*, echinoderms, *Acicularia* sp.) (I2: middle *Juvavites* beds at Tiling; x 25 JS 39). I) Bored and iron-stained mudstone cut by sedimentary dyke (Nimaloksa/Alaror boundary, Hal; x 11 HS 376).

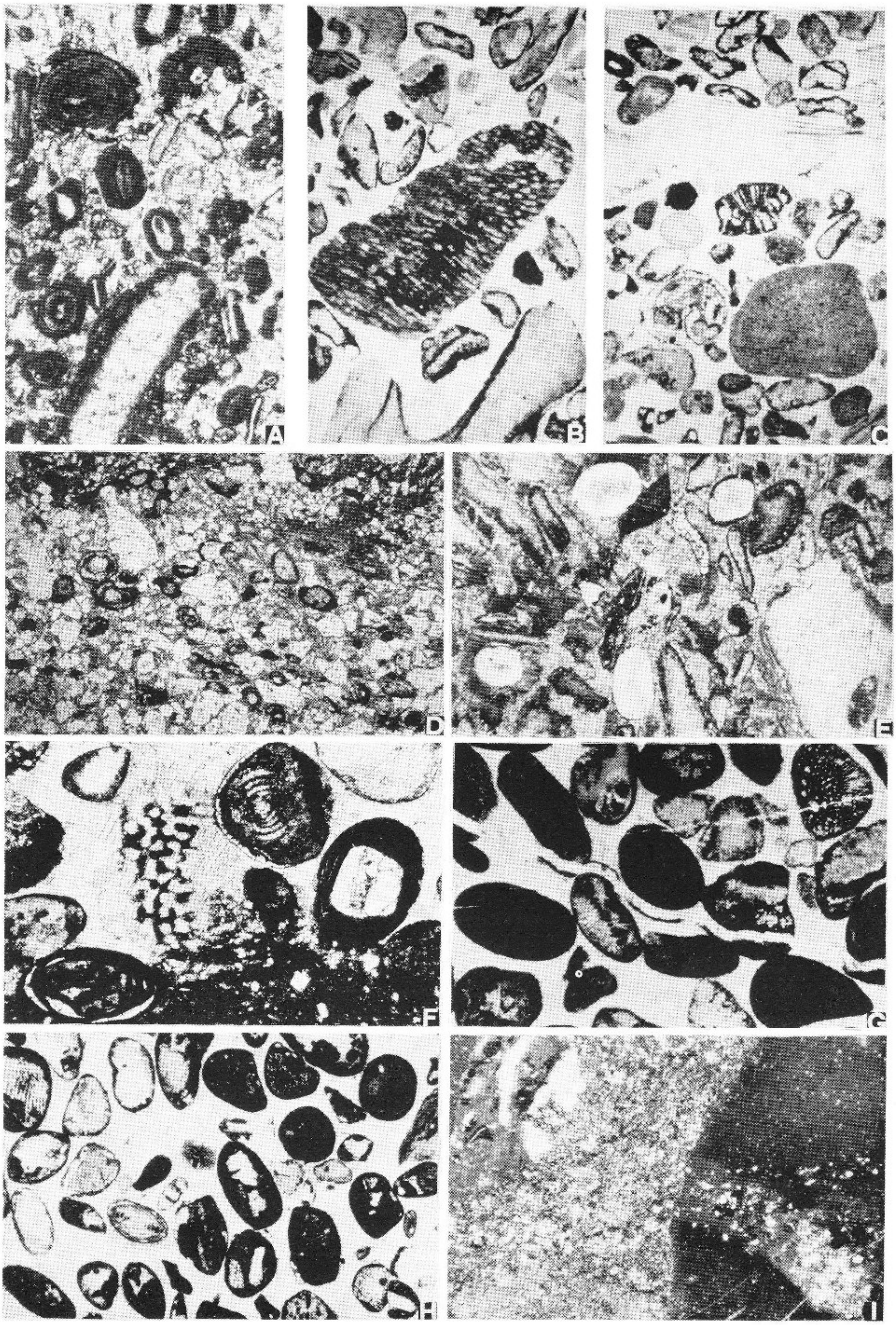
A
B
C
D
E
F
G
H
I

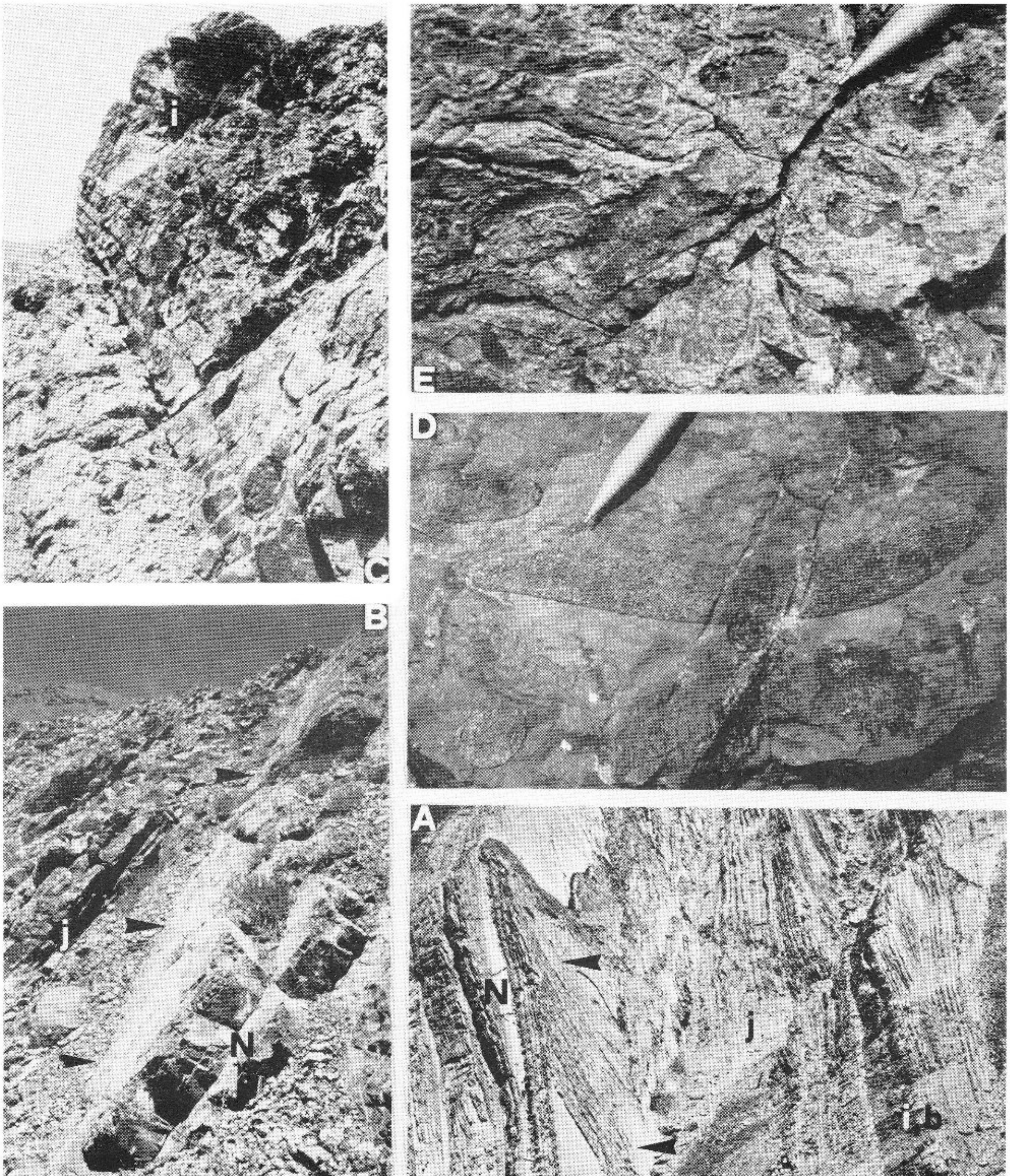

Fig. 13 - Sedimentary features of *Juvavites* beds and Coral limestone. A) Sharp paraconformity (arrows) at top of Nimaloksa Fm. (N) at Muth (j= *Juvavites* beds; i= ironstone shown in C; b= bone bed shown in D). B) Same paraconformity in Parahio valley. C) 11-m thick oolitic ironstone at top of middle *Juvavites* beds at Muth. D) Condensed bone bed with abundant ichthyosaur? ribs at base of upper *Juvavites* beds at Muth (pencil for scale). E) Coral-bearing (arrows) biocalcirudites in the Coral limestone at Muth.

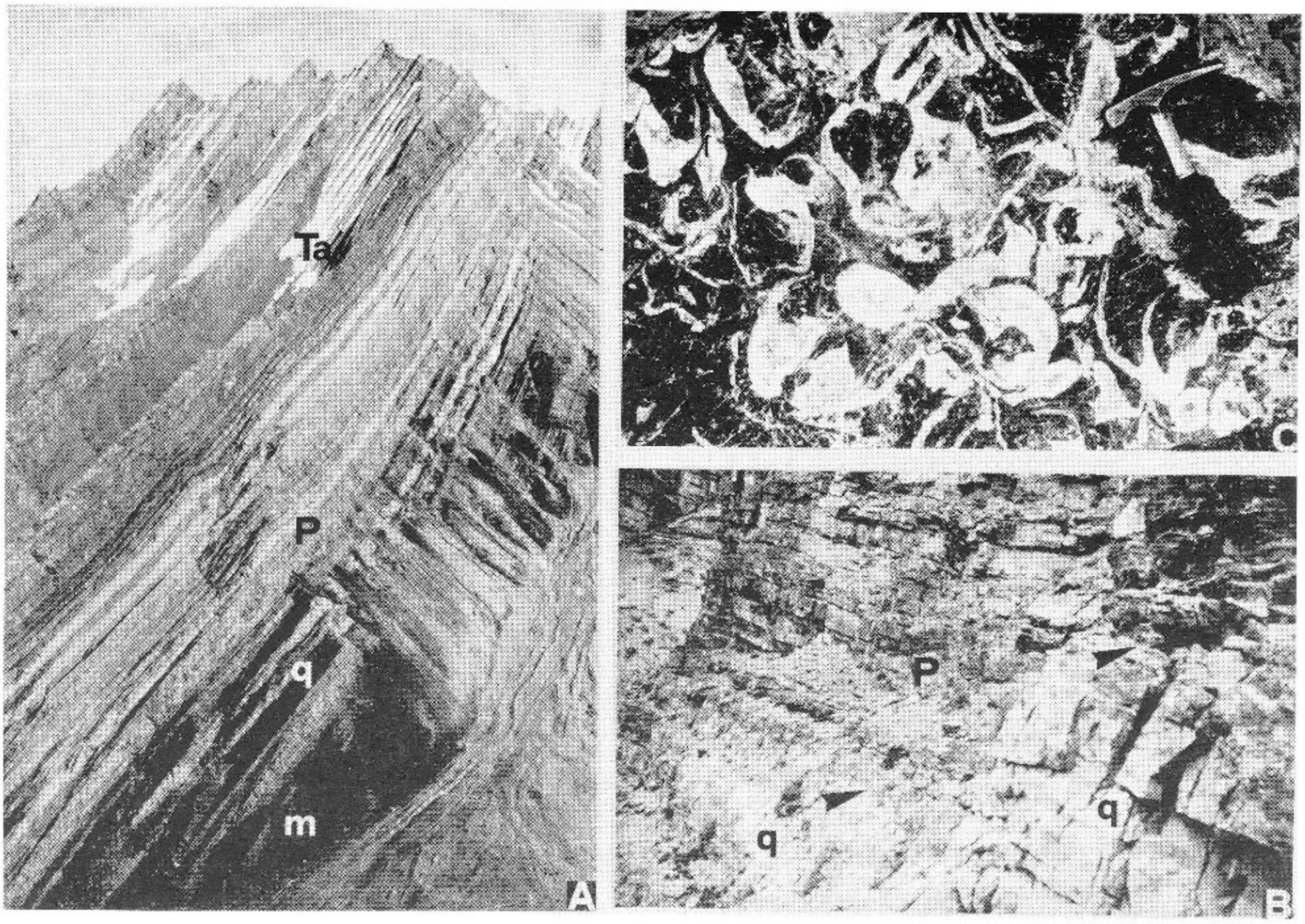

Fig. 14 - Sedimentary features of topmost Alaror to Kioto Groups. A) Boundary at Muth between Alaror Group (m= *Monotis* shale; q= Quartzite series) and light-coloured carbonates of Para Limestone (P), in turn overlain by darker Tagling Limestone (Ta). B) Sharp paraconformable boundary (arrows) at Kioto between Quartzite series and Para Limestone. C) Large megalodontids typical of Para Limestone at Kioto (hammer for scale).

renites with hummocky cross-lamination, burrowed siltstones and hybrid arenites with crinoids, bivalves, gastropods, peloids and locally abundant corals (*"Thecosmilia"* sp.), phosphate nodules, dolomitic lithoclasts and chamositic ooids (I6 in Fig. 7). Next, bioclastic to lithoclastic packstone/rudstones to oolitic grainstones and dolostones commonly displaying ripple to megaripple and herringbone cross-lamination (NW-ward to S-ward paleocurrents) become exclusive (C12 in Fig. 7).

Sedimentary evolution

Tamba Kurkur Formation.

The Permo-Triassic boundary.

The base of the Tamba Kurkur Fm. is a sharp paraconformity (Fig. 15). The Early? Griesbachian is documented in the Spiti valley (Losar, Lingti) and in the lower Pin valley (Guling), where the sedimentation break across the Permian/Triassic boundary is minimum. The hiatus becomes more significant in the Parahio valley (Gechang), where all of the Griesbachian is missing, and even more at Muth, where the Early Dienerian is also absent. Sedimentary gaps of various duration, locally recorded at this stage also in central Nepal (Bassoullet & Colchen, 1977; Nicora, 1991), by no means imply subaerial emergence. They are rather explained with strongly reduced carbonate production as a consequence of the biotic crisis at the end of the Permian, coupled with sediment reworking during a starved deepening stage. Resuspension by intruding oceanic currents in the outer shelf (e.g., Garzanti, 1993) may have prevented sediment accumulation in more proximal settings (upper Pin valley) even for much of the Induan (4.5 Ma according to the Haq et al., 1988 time scale) and possibly also for the whole of the Dorashamian (Bhatt et al., 1980). The centimetric limonitic layer, observed at the base of the Tamba Kurkur Fm. at Lingti (Fig. 15A) but not elsewhere (Fig. 15B; see also Bagati, 1990), is ascribed to superficial alteration (of an originally ferruginous layer?), and not to exposure and

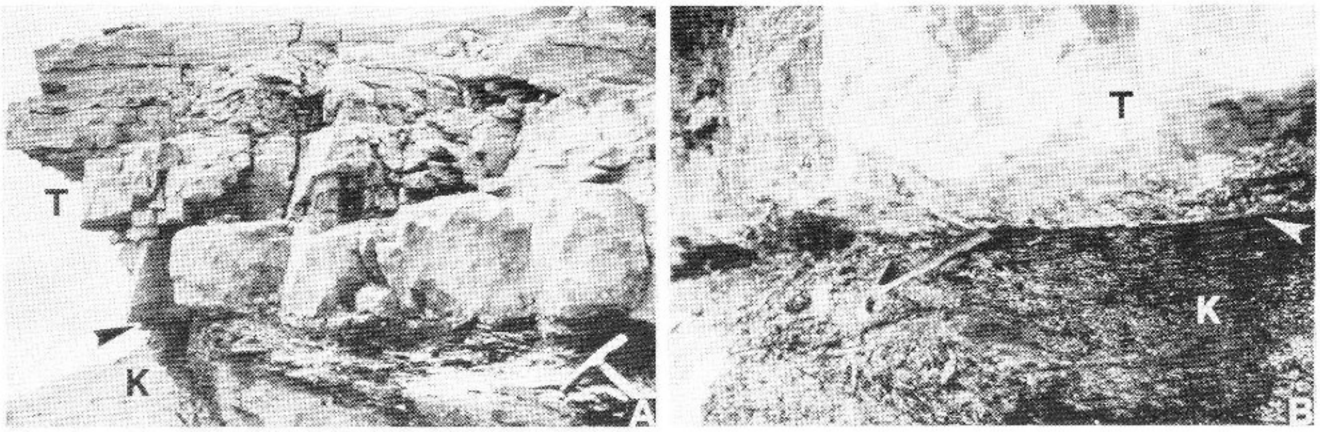

Fig. 15 - Permian/Triassic boundary. A) Sharp paraconformity (arrows) between top of Kuling Group (K) and base of Tamba Kurkur Fm. (T) at Lingti; limonitic layer just above hammer. B) Same paraconformity at Losar, where phosphate nodules occur at base of Tamba Kurkur Fm.

lateritic weathering at the end of the Permian as inferred by Bhatt et al. (1980).

Early Triassic and Anisian.

Condensed limestones with pelagic fauna were deposited on the outer shelf to upper slope during peak transgressive stages. Maximum water depths were probably reached during deposition of the Nodular limestone; pseudo-stromatolitic lamination, best displayed in this limestone band, is ascribed to bacterial mats similar to those forming close to modern shelf-breaks in zones of coastal upwelling (Williams, 1984). Intervals with abundant black mudrocks, which show little burrowing, are instead inferred to have been deposited during regressive stages on offshore middle-shelf bottoms deepening towards the north.

The glauconitic condensed horizon close to the top of the Muschelkalk records another major regional transgression around the Anisian/Ladinian boundary. Similar ironstones were also recognized in Zanskar (our unpubl. data) and Kumaon (Heim & Gansser, 1939). Significant time gaps, recorded at the sharp transition to the Kaga Fm. at Guling, are thought to indicate starvation and prolonged non-deposition in relatively distal settings.

Average accumulation rates, very low for the whole Tamba Kurkur Fm. (2.5 to 4 m/Ma), were even lower for the First limestone band or Muschelkalk and reached 5 to 10 m/Ma only in the more pelitic *Hedenstroemia* beds.

In eastern Zanskar, the Tamba Kurkur Fm. still represents the Induan to Anisian with similar facies; clay supply and thickness increase westward (Nicora et al., 1984; Gaetani et al., 1986). In Nepal and southern Tibet, the Tamba Kurkur Fm. represents instead only the Induan to earliest Aegean (Garzanti et al., 1994a, 1995), with Hanse-type marly facies (Mukut Fm.) beginning as early as the latest Smithian in central Dolpo (Garzanti et al., 1992).

Hanse Group.

The Hanse Group was deposited in deep and low-energy offshore shelf environments, only episodically influenced by storms. A significant increase in clay supply led to only slightly increased accumulation rates for the Kaga marls (about 10 m/Ma), overlain by the Chomule limestones. Renewed clay supply in the late Early Carnian was instead associated with notably increased accumulation rates (around 50 m/Ma).

The Ladinian succession seems to be much thicker in Zanskar, where the lower-middle part of the Hanse Group (240 m) is reported to contain Late Ladinian ammonoids at the top (Baud et al., 1984; Gaetani et al., 1986).

Nimaloksa Formation.

The Lower Member of the Nimaloksa Fm. displays at the base a distinct shallowing-upward trend from mixed carbonate/terrigenous shelf mudrocks to high-energy subtidal calcarenites (CT1 to C3 in Fig. 7), documenting the progradation of a carbonate ramp.

The more terrigenous Middle Member accumulated on subtidal carbonate ramp to open bay storm-dominated settings. Shallow subtidal facies (Muth) passed laterally to deeper-water shelf environments in the north (Parahio valley to Kioto).

The Upper Member, representing a marker horizon in the Spiti-Zanskar Synclinorium (similar thickness and facies characterize the Zozar Fm. in eastern Zanskar; Jadoul et al., 1990, fig. 4), was largely deposited on a shallow-subtidal, high-energy, open-marine carbonate platform, deepening towards the northwest (Parahio valley to Kioto). Peritidal stromatolitic dolostones

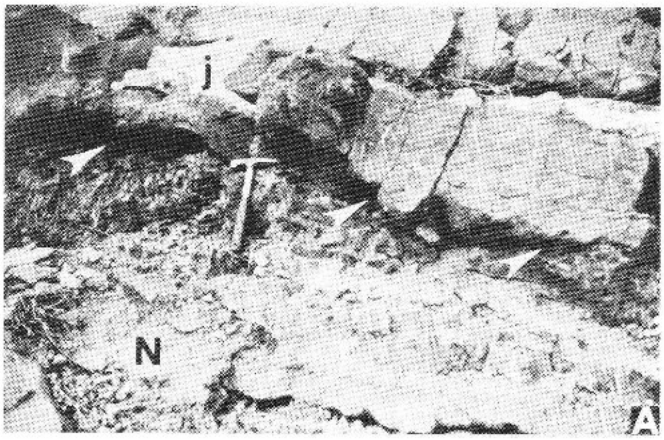

Fig. 16 - Disconformity between Nimaloksa Fm. and Alaror Group. A) Top of Nimaloksa Fm. (N) at Hal is intensely burrowed, penetrated by sedimentary dykes and scoured (arrows) by lenticular breccia containing abundant extraformational carbonate lithoclasts (base of *Juvavites* beds; j) (hammer for scale). B) Base of *Juvavites* beds at Kioto, with carbonate clasts (up to 20 cm in size) derived from the underlying Nimaloksa Fm.

document a regressive event in its lower part (C7 in Fig. 7 and 8).

The paraconformable to disconformable top of the unit, locally testifying to major erosion and extensive development of sedimentary dykes, records a major sedimentary break (Fig. 16). Time involved was probably minor, since very high average subsidence rates are documented by the considerable thickness of the Upper Carnian to Lower Norian succession. Since the top of the Nimaloksa Fm. is characterized by commonly oncolitic subtidal limestones and evidence of regression associated with regional emergence is lacking, an extensional tectonic phase followed by deepening is indicated.

The Nimaloksa Fm. accumulated at greatly increased depositional rates (around 100 m/Ma). Similar thickness characterizes the eastern Zanskar succession, where the upper part of the Hanse Group (lying below the Zozar Fm. and corresponding to the Lower and Upper Members of the Nimaloksa Fm. of Spiti) consists of about 300 m of locally silty mudstones overlying grey marls yielding *Gondolella polygnathiformis* (Jadoul et al., 1990). The great contrast in thickness between the Ladinian/Lower Carnian and Upper Carnian/Lower Norian succession, observed also in central Nepal (Mukut Fm.; Garzanti et al., 1994a, fig.7), has been tentatively ascribed to a stage of renewed tectonic extension (Berra et al., 1993).

Alaror Group.

In the Alaror Group, terrigenous detritus is generally coarser and packstone/grainstones are more common in the Muth area (Fig. 17), whereas the Kioto section mostly consists of siltstones interbedded with mudstone/wackestones, indicating scarce in situ carbonate productivity. Only at the top of the group (Quartzite series) do fine- to medium-grained sandstones become widespread.

The base of the *Juvavites* beds marks a major increase in terrigenous detritus, deposited by storms and tidal currents on a shallow-water shelf. A local erosional event was followed by rapid deepening, as documented by the *lower lithozone*, which accumulated mainly below storm wave-base in middle (Pin valley) to outer (Kioto) shelf environments. The overlying *middle lithozone*, largely deposited above storm wave-base, consists of an overall shallowing-upward sequence capped by a major oolitic ironstone horizon indicating rapid transgression. Similar starvation events are well documented in Zanskar (Garzanti et al., 1989; member a of Jadoul et al., 1990). Condensed bone beds and ammonoids occurring at the base of the *upper lithozone* suggest still reduced detrital input and rapid deepening, followed by sedimentation of exclusive mid-shelf muds.

Terrigenous supply was strongly reduced around the Early/Middle Norian boundary, when the Coral limestone was deposited. Isolated coral knoll reefs developed in cleaner waters onto the Indian passive margin shelf (Bhargava & Bassi, 1985), and passed laterally to coarse bioclastic deposits (Pin valley) and finally to mudstone/wackstones in middle/outer shelf settings (Kioto). Water depth never exceeded some tens of metres in the studied localities, as documented by associated hummocky and bipolar climbing-ripple cross-lamination. Similar patch reefs developed seemingly at the same time in a vast area of the Tethys Himalaya, from Zanskar (Jadoul et al., 1990) and Ladakh (Stutz, 1988) to Nepal (Fuchs et al., 1988).

Fine-grained terrigenous supply resumed at the base of the *Monotis* shale, which accumulated during the Middle Norian on an inner to middle shelf at water depths largely between average-storm and fair-weather wave-base. A shallowing event is indicated by the sharp transition from the *lower lithozone*, locally containing ammonoids, to the largely storm-deposited arenites of

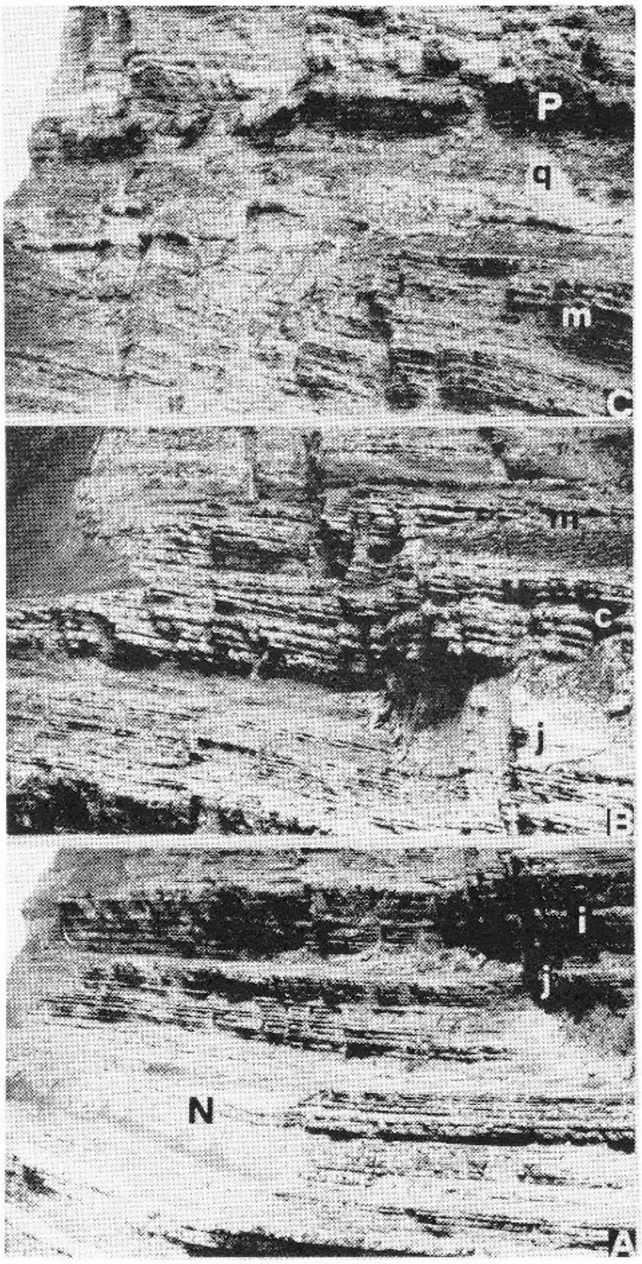

Fig. 17 - The complete section of the Alaror Group at Muth, displaying multiorder cyclicity. A) Thickening-upward sequences in the lower and middle *Juvavites* beds (N= top of Nimaloksa Fm.; i= ironstone in Fig. 13C). B) Coral limestone band (c), occurring between mudrocks of upper *Juvavites* beds (j) and lower *Monotis* shale (m). C) Overall coarsening and shallowing in the middle-upper *Monotis* shale to Quartzite series (q) and Para Limestone (P).

the *middle lithozone*. The occurrence of condensed layers rich in non-carbonate intrabasinal grains (NCI; Garzanti et al., 1989; Garzanti, 1991), including iron ooids, chamosite, phosphate and black grains, documents starvation during rapid sea-level rise in the *upper lithozone*. The *Monotis* shale is broadly equivalent to the upper part of the Tarap Shale in Nepal ("upper assemblage" of Garzanti et al., 1992; "upper member" of Garzanti et al., 1994a).

A major regressive stage at the close of the Norian is recorded by sharp increase in abundance and grain size of quartzo-feldspathic detritus in the overlying Quartzite series, which was sedimented in shallow subtidal to shoreface environments. The unit, recognized in all Tethys Himalayan regions, from Zanskar (member c of Jadoul et al., 1990) to central Nepal and Tibet (Garzanti et al., 1992, 1994a; Jadoul et al., 1995), is thinnest in Spiti.

The Alaror Group was deposited at decreasing accumulation rates, from 50 to 100 m/Ma in the late Early Norian (*Juvavites* beds, Coral Limestone) to about 30 m/Ma in the Middle Norian to mid?-Rhaetian (*Monotis* shale, Quartzite series).

Kioto Group.

Subtidal megalodon-bearing limestones and high-energy tidal calcarenites, still intercalated with quartzo-feldspathic sandstones locally containing dolomite lithoclasts and chamosite ooids, document renewed transgression before the close of the Triassic. Similar facies and thickness are displayed by the Para Limestone in the adjacent Zanskar region (sublithozone a1 of Jadoul et al., 1990). Next, siliciclastic supply stopped and, all along the northern passive continental margin of the Indian subcontinent, platform carbonates accumulated at average rates of only 10 m/Ma, during the Early to early Middle Jurassic (Tagling Limestone; Jadoul et al., 1985, 1990).

Multiorder sequence stratigraphy: cycle hierarchy and interplaying factors

The sedimentary record of continental margins typically consists of long-term sequences (Hubbard et al., 1985; Boote & Kirk, 1989; Bosellini, 1989), each made by nested sets of shorter-term sequences and cyclothems stacked in aggrading, backstepping, infilling and forestepping stratal packages (Van Wagoner et al., 1988; Mitchum & Van Wagoner, 1991).

In the complete Triassic succession of Spiti, well-displayed multiorder cyclicity was controlled by several paleogeographic factors including, besides regional tectonic subsidence and eustatic fluctuations, also climate and latitudinal drift. In spite of abundance of age-diagnostic fossils and extraordinary exposure, stratigraphic information is generally insufficient to unravel in detail the relative incidence of these multiple interacting factors.

Climate and latitudinal drift.

Due to rotation of Gondwana, the Tethys Himalayan margin was progressively and rapidly displaced from the Southern Polar Circle toward the Southern Tropic at the close of the Paleozoic (Dercourt et al., 1993; Ogg & Von Rad, 1994). The Permian terrigenous succession in fact first reflects climatic amelioration (Dickins, 1993; Garzanti et al., 1994b) and next documents increasing aridity at the close of the period (Dutta & Suttner, 1986; Sciunnach & Garzanti, in prep.). Consistent with tropical arid conditions in the Triassic is the much greater abundance of platform carbonates, interbedded at several intervals with arkosic to subarkosic sandstones and commonly containing early authigenic minerals grown in hypersaline environments (feldspars, rare gypsum, bipyramidal quartz).

More humid conditions at lower southern latitudes (about 14°S for Spiti in the Late Norian; Dercourt et al., 1993), may have contributed to increasing terrigenous detritus in the Alaror Group. The platform carbonates of the Kioto Group seem instead to indicate the return to widespread arid tropical conditions, even though available paleomagnetic data and recent paleogeographic reconstructions do not show significant paleolatitude changes from the Late Triassic to the Early Jurassic (Dercourt et al., 1993; Ogg & Von Rad, 1994).

Long-term transgressive/regressive sequences.

At large scale, the Triassic sedimentary succession of the Tethys Himalaya, from the Spiti-Zanskar Synclinorium to central Nepal and southern Tibet (Garzanti et al., 1992, 1994a; Jadoul et al., 1995), records the progressive up- and out-building of the continental terrace of the Northern India passive margin (Gaetani & Garzanti, 1991, fig.7).

The succession is part of a Permo-Jurassic megasequence which, according to the model of Van Wagoner et al. (1988; Duval et al., 1992), can be subdivided into second-order supersequences (Gaetani & Garzanti, 1991, fig.4); these are made in turn by aggrading, backstepping, infilling and forestepping stratal packages (second-order systems tracts), each comprising several third-order "Vail-type" depositional sequences.

After initial opening of the Neotethys Ocean and subsequent rapid transgression driven by rapid thermal subsidence in the Late Permian (second-order "transgressive tract"), the Tethys Himalayan sediments record a sharp transition from offshore shelf to outermost shelf/upper slope environments close to the Permian/Triassic boundary. Abrupt decrease in accumulation rates and widespread prolonged hiatuses are ascribed to strongly reduced carbonate production related to the dramatic P/T biotic crisis and sediment reworking in shelf-break settings (major "condensed section"). Maximum depth is reached during deposition of the Induan to Anisian Tamba Kurkur Fm. (second-order "early highstand tract"), followed by a thick shallowing-upward sequence, represented by the late Early Ladinian to Lower Norian Hanse Group and Nimaloksa Fm. ("late highstand tract"). This trend is in opposition with respect to the long-term eustatic rise drawn on the Haq et al. (1988, fig.17) curve, and thus is not primarily eustatic in nature (accomodation space created by long-term sea-level rise is one order of magnitude less than that provided by subsidence). Rather, it largely reflects progressively increasing terrigenous supply to and carbonate productivity along the shores of Neotethys. Accumulation rates peaked during multi-phase progradation of the Nimaloksa carbonate ramp in the latest Carnian to Early Norian, until peritidal platform conditions were reached at the base of the Upper Member. This stage of rapid sediment accumulation and subsidence ended with an extensional tectonic event, testified locally by a major disconformity at the base of the Alaror Group (II/III supersequence boundary; Gaetani & Garzanti, 1991).

Accumulation rates progressively decreased during sedimentation of the Alaror Group until, during the latest Triassic to Middle Jurassic, slow monotonous deposition of the Kioto platform carbonates reflected the attained stabilization of the Indian continental margin (supersequence III of Gaetani & Garzanti, 1991).

"Vail-type" depositional sequences.

Even though the Tethys Himalaya is a classic passive continental margin succession, seldom are third-order depositional sequences unambiguously distinguished in the field, and the eustatic signal easily inferred from the stratigraphic record.

Index fossils are sufficiently abundant to allow precise correlation with the eustatic cycles drawn on the eustatic chart (Haq et al., 1988) only in the pelagic sediments of the Tamba Kurkur Fm., where cyclic alternation of carbonates and mudrocks is safely interpreted as chiefly controlled by global sea-level changes (Fig. 18).

Lower Triassic and Anisian.

The base of the Tamba Kurkur Fm. is a major omission surface corresponding to the Permian/Triassic boundary, not only in Spiti but all along the Tethys Himalaya. Similar facies are exposed further to the west in the Salt Range, where the global reference section for the latest Permian to Early Triassic depositional sequences was established (Haq et al., 1988, fig.13). According to the Haq et al. model, the P/T boundary corresponds to the transgressive surface of sequence UAA-1.2, possibly coinciding in Spiti, where the Dorashamian was never documented, with the sequence boundary (hence the long debated frequent occurrence of Permian faunas

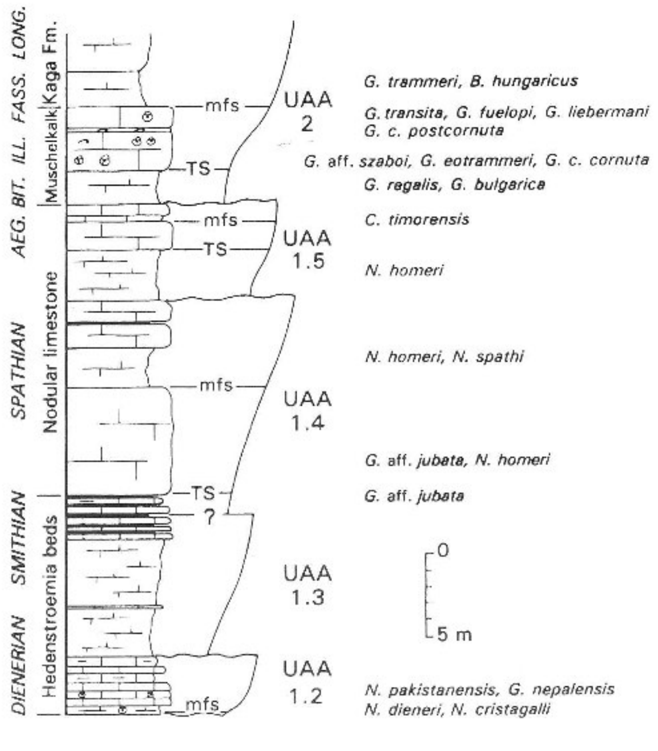

Fig. 18 - Third-order "Vail-type" sequences in the Induan to Early Ladinian succession at Muth (Tamba Kurkur Fm.). Conodont data from Spiti document good overall correspondence with global eustatic cycles (Haq et al., 1988; Hirsch, 1994, fig. 4, 5). Sequences UAA-1.3 and UAA-2.1 are poorly constrained biostratigraphically; the transgressive tract of sequence UAA-1.2 is documented only in the lower Pin and Spiti valleys (Fig. 3). TS= transgressive surface; mfs= maximum flooding surface.

at the base of the *Otoceras* beds; Bhatt & Arora, 1984; Orchard et al., 1994; Atudorei et al., 1995).

The First limestone band and Nodular limestone correlate well (at conodont zone level) with transgressive system tracts of sequences UAA-1.2 and UAA-1.4, drawn on the Haq et al. (1988) chart and recognized worldwide (Hirsch, 1994; Moerk, 1994; Paull & Paull, 1994). Only the Smithian transgression (sequence UAA-1.3), much better documented in central Nepal (Garzanti et al., 1992, 1994a), is difficult to detect within the rather homogeneous and conodont-poor *Hedenstroemia* beds. The glauconitic greensand in the upper Muschelkalk records another major Tethyan transgression around the Anisian/Ladinian boundary (Hirsch, 1994).

On the other hand, shaly intervals occurring all along the Tethys Himalaya in the Upper Dienerian, Upper Smithian, Lower Aegean and Illyrian correlate well with regressive stages (Hirsch, 1994, fig. 4, 5). Even though such eustatic cyclicity is well-displayed, sequence boundaries are invariably subtle and very difficult to detect in the field. According to the Haq et al. (1988) model, only the base of mudrock intervals, where limestones are still intercalated, represents the highstand tract, whereas the upper part, where black shales become predominant, documents the lowstand systems tract of the overlying sequence.

Ladinian.

Even though biostratigraphic control is poor, similar third-order mudrock/carbonate sequences may be recognized also in the Hanse Group. Correlation with the Haq et al. (1988) chart would suggest that increasing clay supply documented in the Kaga marls took place during the long Late Ladinian regression (highstand of sequence UAA-2.2 to lowstand of sequence UAA-3.1), whereas the predominant limestones of the Chomule Fm. accumulated across the Ladinian/Carnian boundary during the transgressive part of sequence UAA-3.1.

Upper Triassic.

Correlation with the Haq et al. (1988) chart would indicate that renewed clay supply documented by the Grey beds began during the late Early Carnian highstand of sequence UAA-3.1 and continued in sequence UAA-3.2. The overlying Lower Member of the Nimaloksa Fm., confined to the latest Carnian and containing the Carnian/Norian boundary at the top, would correlate with the lowstand to transgressive tracts of sequence UAA-4, the long highstand tract of which would include the Middle and Upper Members of the Nimaloksa Fm. and most of the Alaror Group as well (*Juvavites* beds to *Monotis* shale). The regressive Quartzite series would document the lowstand tract of sequence UAB-1, with the topmost Triassic basal part of the Kioto Group representing the transgressive to highstand tracts of sequence UAB-1 and the lowstand of the overlying sequence UAB-2.

In fact, due to markedly increased accumulation rates, a much greater number of third- to fourth-order sequences can be recognized in the Upper Triassic succession of Spiti (Fig. 19). However, for the rather low definition of the Haq et al. (1988) curve in this epoch, it is difficult to evaluate the relative incidence of eustatism and other geological factors in controlling the sedimentary record.

Third- to fourth-order sequences in the Grey beds and Nimaloksa Formation.

Several pluridecametric regressive/transgressive sequences are recognized in the Grey beds (four marl/marly limestone sequences), and in the Lower Member (two major shallowing-upward sequences capped by platform carbonates: C1 and C3 in Fig. 19) to Middle Member of the Nimaloksa Formation (two shallowing-upward sequences beginning with silty mudrocks: T2 and T5 in Fig. 19). Next, the Upper Member records a sharp regressive event in its lower part (C7

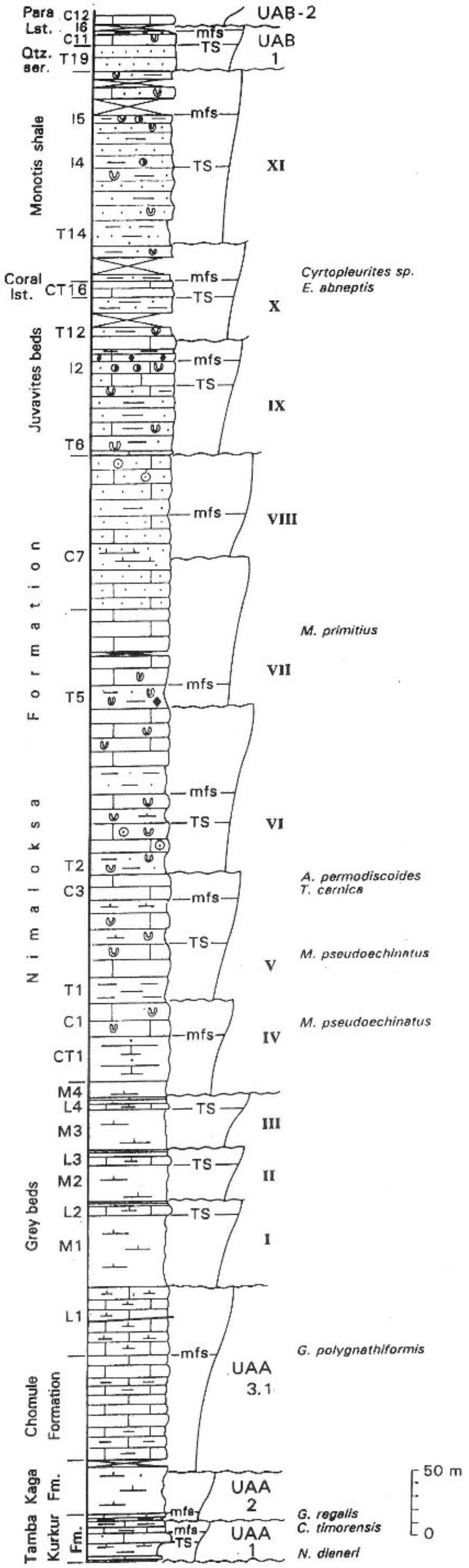

in Fig. 19) and a major tectonically-related disconformity at its top. Though both of these are good candidates for a sequence boundary, none is drawn at this stage in the Haq et al. (1988) chart.

Third- to fourth-order sequences in the Alaror Group.

Three regressive/transgressive sequences are particularly well-displayed in the *Juvavites* beds to *Monotis* shale. Lowstand tracts are characterized by marly and silty to sandy coarsening-upward sequences, locally displaying basal scoured base (T6-9, T12, T14-15-16 in Fig. 7, 8, 19); high-energy biocalcarenites, locally with a ravinement surface at the base, represent the overlying transgressive tract (C9, CT16: Coral Limestone, CT20). Condensed horizons are marked by NCI-bearing arenites to oolitic ironstones (I2, I3, I5), followed by extensively burrowed downlap surfaces and phosphatic beds commonly containing ammonoids or vertebrate bones; the highstand tract is represented by marly shales, frequently poorly exposed (T10-11, T13, T18 in Fig. 7, 8).

Since the overlying Quartzite series and base of Para Limestone document cyclicity at the same scale (T19: lowstand tract; C11: transgressive tract; I6: condensed section), it seems reasonable to assume that most of the recognized sequences are in fact third-order depositional sequences, even though not recognized in the Haq et al. (1988) chart.

"Milankovitch-type" high-frequency cyclothems.

Within the Triassic succession of Spiti, high-frequency cyclothems are well-displayed in several stratigraphic intervals.

In the *Hedenstroemia* beds of the Tamba Kurkur Fm., for example, rhythmically alternating 10 to 15 cm-thick wackestone beds, thin-bedded limestones with shale drapes and 5 to 7 cm-thick black shales, reproduce at decimetric scale the same sedimentary pattern shown by the formation as a whole.

In the Nimaloksa Fm., 1 to 4 m-thick marl to marly silt/limestone cyclothems at the base of the Lower Member (CT1 in Fig. 19) also reproduce at metric scale the same shallowing-upward cycles displayed at pluridecametric scale within the unit. In the Middle Member, metric to decametric shallowing-upward sequences commonly display extensively burrowed tops

Fig. 19 - Third- to fourth-order sequences in the Triassic succession at Muth (see Fig. 7). In the mid-Carnian to mid-Norian (Grey beds to *Monotis* shale), eleven third-order cycles are recognized instead of the two (UAA-3.2 and UAA-4) drawn on the Haq et al. (1988) chart. TS= transgressive surface; mfs= maximum flooding surface.

(Fig. 10B), hinting at significant time gaps (even though well below biostratigraphic resolution).

In the *Juvavites* beds, burrowed silty limestone/marl decimetric bed couplets reflect highest-frequency cyclicity, superposed to metric thickening-upward cyclothems, arranged in turn in decametric shallowing-upward sequences (Fig. 17A).

Such variety of nested 4th to 5th-order cycles (PACs or parasequences; Goodwin & Anderson, 1985; Mitchum & Van Wagoner, 1991) is common in any sedimentary succession. Even though biostratigraphic evidence is generally inadequate, high-frequency repetition of sedimentary patterns is commonly ascribed to climatic fluctuations driven by orbital changes, controlling in turn the nature and amount of sediment supply.

Conclusions

Thermal subsidence of the newly-formed Indian passive continental margin began after break-up and initial opening of Neotethys in the mid-Permian. The Permian/Triassic bòundary represents a major break in sedimentation, with time gaps from a few Ma to several Ma.

In the Induan to Anisian, the Tamba Kurkur Fm. mainly recorded global eustatic changes, with transgressive stages characterized by nodular limestone sedimentation on the outermost shelf/uppermost slope and regressive stages marked by mudrock deposition on the continental shelf. A glauconitic condensed horizon developed at the Anisian/Ladinian boundary, and the top of the formation reaches the Early Ladinian in relatively proximal settings (Muth).

Due to greater clay supply at the close of the Early Ladinian, accumulation rates increased only slightly in the lower part of the Hanse Group (Kaga marls and Chomule limestones). Another increase in clay supply occurred in the late Early Carnian (Grey beds).

A rapid acceleration of subsidence took place in the Late Carnian/Early Norian, when accumulation rates approached 100 m/Ma even in less subsident proximal parts of the Spiti continental margin (Fig. 20), which deepened towards the north as documented by facies distribution patterns in the Nimaloksa Fm. and Alaror Group. Widespread occurrence of oncoids, coated grains and bored bioclasts nevertheless suggests rather slow sediment burial from the Lower Member of the Nimaloksa Fm. to the Para Limestone (Fig. 9 and 12), with prolonged starvation during flooding stages documented by concentration of iron ooids, blackened grains, chamosite and phosphate (Fig. 12B to H).

The Nimaloksa Fm. displays cyclical carbonate/terrigenous sedimentation on a subtidal carbonate

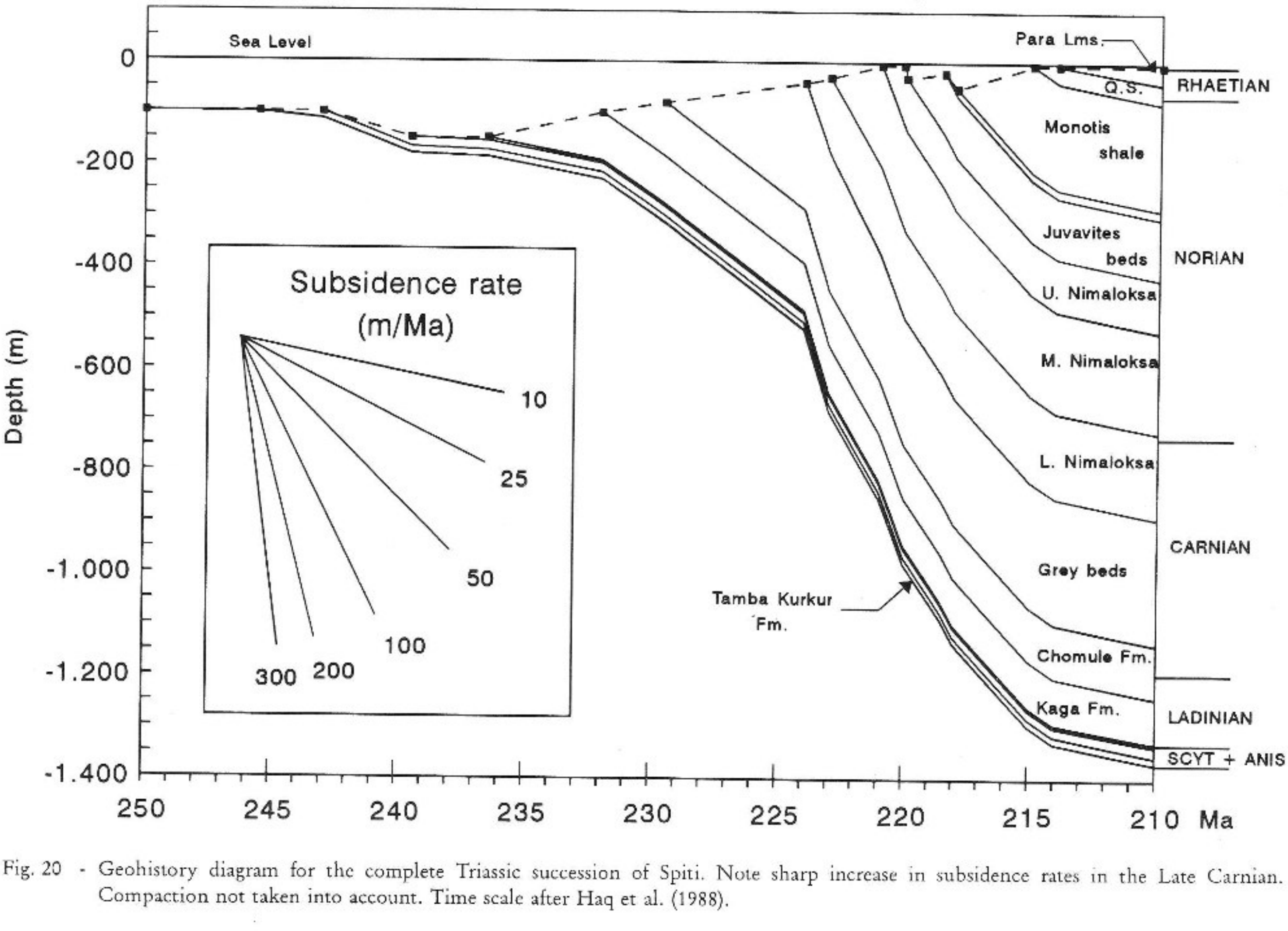

Fig. 20 - Geohistory diagram for the complete Triassic succession of Spiti. Note sharp increase in subsidence rates in the Late Carnian. Compaction not taken into account. Time scale after Haq et al. (1988).

ramp; five third- to fourth-order pluridecametric sequences are recognized (Fig. 19). Progradation of a carbonate ramp in the latest Carnian (Lower Member) was followed by largely terrigenous storm-deposited subtidal sediments in the earliest Norian (Middle Member), and finally by high-energy platform carbonates in the Early Norian (Upper Member). A major disconformity at the top of the unit, locally marked by erosion with development of sedimentary dykes, points to an extensional tectonic event followed by rapid submergence.

An increase in quartzo-feldspathic terrigenous detritus since the late Early Norian is recorded by the Alaror Group, where another four third- to fourth-order pluridecametric sequences are distinguished. Mid-shelf muds and storm-deposited arenites are overlain by tidal biocalcarenites; next, rapid transgression is marked by an oolitic ironstone followed by bone beds and predominating mudrocks (*Juvavites* beds). Another major transgression, associated with starvation characterized by local development of coral patch reefs, is recorded around the Early/Middle Norian boundary (Coral limestone). The Middle Norian begins with mudrocks yielding ammonoids, intercalated higher up with storm-dominated sandstones and hybrid arenites bearing chamosite-goethite ooids, marking regressive and transgressive stages respectively (*Monotis* shale). A major regression in the Late Norian was associated with increase in grain-size of quartzose terrigenous detritus (Quartzite series).

Renewed transgression with gradual disappearance of siliciclastics occurred in the mid?-Rhaetian (Para Limestone), while accumulation rates progressively began to decrease (Tagling Limestone).

Acknowledgments.

Roberto Rettori (Perugia) gave valuable help in determination of Late Triassic benthic foraminifers and biostratigraphic interpretation. Marco Balini determined Norian ammonoids. Topmost Permian to Norian conodont taxonomy was discussed at length with S. Kovacs (Budapest), H. Kozur (Budapest) and M. J. Orchard (Vancouver). We exchanged views on the Permo-Triassic boundary in the field with Trilochan Singh. The manuscript has benefitted from careful reviews by A. J. Boucot (Cornvallis), G. Fuchs (Vienna), M. J. Orchard (Vancouver) and Maurizio Gaetani. Thanks are also due to Curzio Malinverno, Magda Minoli and Giovanni Chiodi for carefully-made thin sections, drawings and photographs. The expedition, partly supported by Ev-K^2-CNR, was carried to complete success by the experience of our guide Rahoul, driver Balwinder Singh and Dawa sherpa. Printing expenses covered by Progetto Coordinato CNR "Ritmi ed Eventi in Biostratigrafia" (Coord. Prof. A. Farinacci - Resp. Sc. Prof. M. Tongiorgi).

REFERENCES

Atudorei V., Baud A. & Sharp Z.D. (1995) - Late Permian and Early Triassic carbon isotope and sequence stratigraphy of the Northern Indian margin. *X Himalaya - Tibet - Karakorum Workshop*, Abstract volume, Ascona.

Bagati T.N. (1990) - Lithostratigraphy and facies variation in the Spiti Basin (Tethys), Himachal Pradesh, India. *Journ. Himal. Geol.*, v.1, pp. 35-47, Dehra Dun.

Bassoullet J.P. & Colchen M. (1977) - La limite Permien-Trias dans le domaine tibétain de l' Himalaya du Nepal (Annapurnas-Ganesh Himal). *Coll. Int. C.N.R.S.*, n. 268, pp. 41-52, Paris.

Baud A., Gaetani M., Garzanti E., Fois E., Nicora A. & Tintori A. (1984) - Geological observations in southeastern Zanskar and adjacent Lahul area (northwestern Himalaya). *Ecl. Geol. Helv.*, v. 77, n. 1, pp. 171-197, Basel.

Berra F., Jadoul F., Garzanti E. & Nicora A. (1993) - Stratigraphic and paleogeographic evolution of the Carnian-Norian succession of the Spiti region (Tethys Himalaya, India), *VIII Himalaya - Tibet - Karakorum Workshop*, Abstract volume, pp. 59-61, Wien.

Bhargava O.N. (1987) - Stratigraphy, microfacies and palaeoenvironment of the Lilang Group (Scythian - Dogger), Spiti Valley, Himachal Himalaya, India. *Journ. Paleont. Soc. India*, v. 32, pp. 92-107, Lucknow.

Bhargava O.N. & Bassi U.K. (1985) - Upper Triassic coral knoll reefs: Middle Norian, Spiti-Kinnaur, Himachal Himalaya, India. *Facies*, v. 12, pp. 219-242, Erlangen.

Bhargava O.N. & Gadhoke S.K. (1988) - Triassic microfauna of the Lilang Group with special reference to Scythian-Anisian conodonts, Spiti Valley, Himachal Himalaya. *Journ. Geol. Soc. India*, v. 32, pp. 494-505, Lucknow.

Bhatt D.K. & Arora R.K. (1984) - *Otoceras* bed of Himalaya and Permian-Triassic boundary - assessment and elucidation with conodont data. *Journ. Geol. Soc. India*, v. 25, pp. 720-727, Lucknow.

Bhatt D.K., Fuchs G., Prashara K.C., Krystyn L., Arora R.K. & Golebiowski R. (1980) - Additional ammonoid layers in the Upper Permian sequence of Spiti. *Bull. Ind. Geol. Ass.*, v. 13, pp. 57-61, Chandigar.

Boote D.R.D. & Kirk R.B. (1989) - Depositional wedge cycles on evolving plate margins, Western and Northwestern Australia. *Am. Ass. Petr. Geol. Bull.*, v. 73, pp. 216-243, Tulsa.

Bosellini A. (1989) - The continental margins of Somalia: Their structural evolution and sequence stratigraphy. *Mem. Sc. Geol.*, v. 41, pp. 373-458, Padova.

Dercourt J., Ricou R.E. & Vrielinck B. (1993) - Atlas Tethys Palaeoenvironmental maps. Gauthier-Villars, pp. 9-80, Paris.

Dickins J.M. (1993) - Climate of the Late Devonian to Triassic. *Palaeogeogr., Palaeoclim., Palaeoecol.*, v. 100, pp. 89-94, Amsterdam.

Diener C. (1908) - Ladinic, Carnic and Noric faunae of Spiti. *Palaeont. Indica*, s. 15, v. 5, Mem. 3, 157 pp., Calcutta.

Diener C. (1912) - The Trias of the Himalayas. *Mem. Geol. Soc. India*, v. 36, pp. 1-176, Lucknow.

Dutta P.K. & Suttner L.J. (1986) - Alluvial sandstone composition and paleoclimate. II Authigenic mineralogy. *Journ. Sedim. Petrol.*, v. 56, pp. 346-358, Tulsa.

Duval B., Cramez C. & Vail P.R. (1992) - Types and hierarchy of stratigraphic cycles. Sequence stratigraphy of European Basins. Abstract volume, p. 44, Dijon.

Fuchs G. (1982) - The geology of the Pin valley in Spiti, H.P., India. *Jahrb. Geol. Bundesanst.*, v. 124, n. 2, pp. 325-359, Wien.

Fuchs G. (1987) - The geology of southern Zanskar (Ladakh) - evidence for the autochthony of the Tethys Zone of the Himalaya. *Jahrb. Geol. Bundesanst.*, v. 130, n. 4, pp. 465-491, Wien.

Fuchs G., Widder R.W. & Tuladhar R. (1988) - Contributions to the geology of the Annapurna Range (Manang area, Nepal). *Jahrb. Geol. Bundesanst.*, v. 131, n. 4, pp. 593-607, Wien.

Gaetani M., Casnedi R., Fois E., Garzanti E., Jadoul F., Nicora A. & Tintori A. (1986) - Stratigraphy of the Tethys Himalaya in Zanskar, Ladakh. *Riv. It. Paleont. Strat.*, v. 91 (1985), n. 4, pp. 443-478, Milano.

Gaetani M. & Garzanti E. (1991) - Multicyclic history of the northern India continental margin (NW Himalaya). *Am. Ass. Petr. Geol. Bull.*, v. 75, pp. 1427-1446, Tulsa.

Garzanti E. (1991) - Non-carbonate intrabasinal grains in arenites: their recognition, significance and relationship to eustatic cycles and tectonic setting. *Journ. Sedim. Petrol.*, v. 61, n. 6, pp. 959-975, Tulsa.

Garzanti E. (1993) - Sedimentary evolution and drowning of a passive margin shelf (Giumal Group; Zanskar Tethys Himalaya, India): palaeoenvironmental changes during final break-up of Gondwanaland. In Treloar P.J. & Searle M.P. (Eds.) - Himalayan tectonics. *Geol. Soc.*, Spec. Publ. 74, pp. 277-298, London.

Garzanti E., Angiolini L. & Sciunnach D. (in prep.) - Stratigraphy of the Permian Kuling Group (Spiti, Lahul and Zanskar; NW Himalaya): sedimentary evolution during opening of Neo-Tethys.

Garzanti E., Haas R. & Jadoul F. (1989) - Ironstones in the Mesozoic passive margin sequence of the Tethys Himalaya (Zanskar, Northern India): sedimentology and metamorphism. In Young T.P. & Taylor W.E.G. (Eds.) - Phanerozoic ironstones. *Geol. Soc.*, Spec. Publ. 46, pp. 229-244, London.

Garzanti E., Nicora A., Sciunnach D. (1995) - The Permian-Triassic boundary and the Lower Triassic in the Tethys Himalaya of Southern Tibet - Preliminary report. *X Himalaya - Tibet - Karakorum Workshop*, Abstract volume, Ascona.

Garzanti E., Nicora A. & Tintori A. (1992) - Late Paleozoic to Early Mesozoic stratigraphy and sedimentary evolution of central Dolpo (Nepal Himalaya). *Riv. It. Paleont. Strat.*, v. 98, n. 3, pp. 271-298, Milano.

Garzanti E., Nicora A. & Tintori A. (1994a) - Triassic stratigraphy and sedimentary evolution of the Annapurna Tethys Himalaya (Manang area, Central Nepal). *Riv. It. Paleont. Strat.*, v. 100, n. 2, pp. 195-226, Milano.

Garzanti E., Nicora A., Tintori T., Sciunnach D. & Angiolini L. (1994b) - Late Paleozoic stratigraphy and petrography of the Thini Chu Group (Manang, Central Nepal): sedimentary record of Gondwana glaciation and rifting of Neotethys. *Riv. It. Paleont. Strat.*, v. 100, n. 2, pp. 155-194, Milano.

Goel R.K. (1977) - Triassic Conodonts from Spiti (H.P.), India. *Journ. Paleont.*, v. 51, n. 6, pp. 1085-1101, Tulsa.

Goodwin P.W. & Anderson E.J. (1985) - Punctuated aggradational cycles: a general hypothesis of episodic stratigraphic accumulation. *Journ. Geol.*, v. 93, pp. 515-533, Chicago.

Haq B.U., Hardenbol J. & Vail P.R. (1988) - Mesozoic and Cenozoic chronostratigraphy and cycles of sea-level change. In Wilgus C.K. et al. (Eds.) - Sea-level changes - an integrated approach. *Soc. Econ. Paleont. Min.*, Spec. Publ. 42, pp. 71-108, Tulsa.

Hayden H.H. (1904) - The geology of Spiti, with parts of Bashar and Rupshu. *Mem. Geol. Surv. India*, v. 36, pp. 1-129, Calcutta.

Hayden H.H. (1908) - Geography and geology of the Himalaya (Part 4). *Geol. Surv. India*, pp. 233-236, Calcutta.

Heim A. & Gansser A. (1939) - Central Himalaya. Geological observations of the Swiss expedition 1936. *Mem. Soc. Helv. Sc. Nat.*, v. 73, n. 1, 246 pp., Zürich.

Hirsch F. (1994) - Triassic multielement conodonts versus eustatic cycles. In Guex J. & Baud A. (Eds.) - Recent developments on Triassic stratigraphy. *Mém. Géol.*, n. 22, pp. 35-51, Lausanne.

Hubbard R.J., Pape J. & Roberts D.G. (1985) - Depositional sequence mapping to illustrate the evolution of a passive continental margin. In Berg O.R. & Woolverton D.G. (Eds.) - Seismic stratigraphy II - An integrated approach. *Am. Ass. Petr. Geol.*, Mem. 39, pp. 93-115, Tulsa.

Jadoul F., Berra F., Garzanti E. & Sciunnach D. (1995) - The sedimentary succession of the Southern Tibet Tethys Himalaya - Initial report and preliminary comparisons with central Nepal and Northern India - Part 2: Mesozoic. *X Himalaya - Tibet - Karakorum Workshop*, Abstract volume, Ascona.

Jadoul F., Fois E., Tintori A. & Garzanti E. (1985) - Preliminary results on Jurassic stratigraphy in Zanskar (NW Himalaya). *Rend. Soc. Geol. It.*, v. 8, pp. 9-13, Roma.

Jadoul F., Garzanti E. & Fois E. (1990) - Upper Triassic/Lower Jurassic stratigraphy and palaeogeographic evolution of the Zanskar Tethys Himalaya (Zangla Unit). *Riv. It. Paleont. Strat.*, v. 95 (1989), n. 4, pp. 351-396, Milano.

Jadoul F. & Sartorio D. (1990) - Preliminary results on the Upper Triassic-Jurassic stratigraphy in the Zumlung-Khurna units (Zanskar Range). *V Himalaya - Tibet - Karakorum Workshop*, Abstract volume, pp. 25-26, Ascona.

Kovacs S. & Kozur H. (1980) - Stratigraphische Reichweite der wichtigsten Conodonten (ohne Zahnreihenconodonten) der Mittel- und Obertrias. *Geol. Paläont. Mitt.*, v. 10, pp. 47-78, Innsbruck.

Kovacs S., Nicora A., Szabo I. & Balini M. (1990) - Conodont biostratigraphy of Anisian/Ladinian boundary sections in the Balaton upland (Hungary) and in the

Southern Alps (Italy). *Courier Forsch. Inst. Senckenberg*, v. 118, pp. 171-195, Frankfurt.

Kozur H. (1989a) - Significance of events in conodont evolution for the Permian and Triassic stratigraphy. *Courier Forsch. Inst. Senckenberg*, v. 117, pp. 385-408, Frankfurt.

Kozur H. (1989b) - The taxonomy of the gondolellid conodonts in the Permian and Triassic. *Courier Forsch. Inst. Senckenberg*, v. 117, pp. 409-469, Frankfurt.

Krystyn L. (1980) - Stratigraphy of the Hallstatt region. In Schönlaub H.P. (Ed.) - 2nd European Conodont Symp., Guidebook and abstracts. *Abhandl. Geol. Bundesanst.*, v. 35, pp. 61-98, Wien.

Krystyn L. (1983) - Das Epidauros-Profil (Griechenland) - ein Beitrag zur Conodonten-Standardzonierung des tethyalen Ladin und Unterkarn. In Zapfe H. (Ed.) - Das Forschungsproject "Triassic on Tethys realm" (IGCP Proj. 4). *Schr. Erdwiss. Komm., Öster. Akad. Wiss.*, v. 5, pp. 231-258, Wien.

Matsuda T. (1985) - Late Permian to early Triassic conodont paleobiogeography in the "Tethys Realm". In Nakazawa K. & Dickins J.M. (Eds.) - The Tethys - Her paleogeography and paleobiogeography from Paleozoic to Mesozoic. *Tokai Univ. Press*, pp. 157-170, Tokyo.

Mitchum R.M. & Van Wagoner J.C. (1991) - High-frequency sequences and their stacking patterns: sequence-stratigraphic evidence of high-frequency eustatic cycles. *Sedim. Geol.*, v. 70, pp. 131-160, Amsterdam.

Moerk A. (1994) - Triassic transgressive-regressive cycles of Svalbard and other Arctic areas: a mirror of stage subdivision. In Guex J. & Baud A. (Eds.) - Recent developments on Triassic stratigraphy. *Mém. Géol.*, n. 22, pp. 69-81, Lausanne.

Nicora A. (1992) - Conodonts from the Lower Triassic sequence of central Dolpo, Nepal. *Riv. It. Paleont. Strat.*, v. 97 (1991), n. 3-4, pp. 239-268, Milano.

Nicora A., Gaetani M. & Garzanti E. (1984) - Late Permian to Anisian in Zanskar (Ladakh Himalaya). *Rend. Soc. Geol. It.*, v. 7, pp. 27-30, Roma.

Ogg J.G. & Von Rad U. (1994) - The Triassic of the Thakkhola (Nepal). II. Paleolatitudes and comparison with other eastern Tethyan margins of Gondwana. *Geol. Rundsch.*, v. 83, pp. 107-129, Stuttgart.

Orchard M.J. (1991a) - Late Triassic conodont biochronology and biostratigraphy of the Kunga Group, Queen Charlotte Islands, British Columbia. In Evolution and hydrocarbon potential of the Queen Charlotte Basin, British Columbia. *Geol. Surv. Canada*, Paper 90-10, pp. 173-193, Vancouver.

Orchard M.J. (1991b) - Upper Triassic conodont biochronology and new index species from the Canadian Cordillera. *Geol. Surv. Canada Bull.*, v. 417, pp. 299-335, Vancouver.

Orchard M.J., Nassichuk W.W. & Rui L. (1994) - Conodonts from the Lower Griesbachian *Otoceras latilobatum* bed of Selong, Tibet, and the position of the Permian-Triassic boundary. In Pangea: global environments and resources. *Canad. Soc. Petr. Geol.*, Mem. 17, pp. 823-843, Calgary.

Pant P.C. & Azmi R.J. (1982) - A record of ostracodes from the Middle Triassic of Spiti, Himachal Pradesh. *Himal. Geol.*, v. 12, pp. 444-448, Dehra Dun.

Paull R.K. & Paull R.A. (1994) - Transgressive conodont faunas; opportunity for sequence recognition and correlation in Lower Triassic strata of the Tethys and Circum-Pacific. *Meeting Shallow Tethys 4*, Abstract, Albrechtsberg.

Sciunnach D. & Garzanti E. (in press) - Sedimentary record of Late Paleozoic rift and break-up in Northern Gondwana (Thini Chu Group and Tamba-Kurkur Fm.; Dolpo Tethys Himalaya, Nepal). *Geodinamica Acta*, Paris.

Srikantia S.V. (1981) - The lithostratigraphy, sedimentation and structure of Proterozoic-Phanerozoic Formations of Spiti basin in the Higher Himalaya of Himachal Pradesh, India. In Sinha A.K. (Ed.) - Contemporary geoscientific researches in Himalaya, v.1, pp. 31-48, Dehra Dun.

Srikantia S.V., Ganesan T.M., Rao P.N., Sinha P.K. & Tirkey B. (1980) - Geology of Zanskar area, Ladakh Himalaya. *Himal. Geol.*, v. 8, pp. 1009-1033, Dehra Dun.

Stoliczka A. (1866) - Summary of the geological observations during a visit to the provinces Rupshu Karnag, South Ladakh, Zanskar, Sumdo and Dras of western Tibet. *Mem. Geol. Surv. India*, v. 5, pp. 337-354, Calcutta.

Stutz E. (1988) - Géologie de la chaîne de Nyimaling aux confins du Ladakh et du Rupschu (NW-Himalaya, Inde) - Evolution paléogéographique et tectonique d' un segment de la marge nord-indienne. *Mém. Géol.*, n. 3, 149 pp., Lausanne.

Sweet W.C. (1988a) - A quantitative conodont biostratigraphy for the Lower Triassic. *Senckenb. Lethaea*, v. 69, n. 3/4, pp. 253-273, Frankfurt.

Sweet W.C. (1988b) - The conodonta: morphology, taxonomy, palaeoecology and evolution history of a long-extinct animal phylum. *Mon. Geol. Geophys.*, n. 10, 212 pp., Oxford.

Van Wagoner J.C., Posamentier H.W., Mitchum R.M., Vail P.R., Sarg J.F., Loutit T.S. & Hardenbol J. (1988) - An overview of the fundamentals of sequence stratigraphy and key definitions. In Wilgus C.K. et al. (Eds.) - Sea-level changes - an integrated approach. *Soc. Econ. Paleont. Min.*, Spec. Publ. 42, pp. 39-45, Tulsa.

Williams L.A. (1984) - Subtidal stromatolites in Monterey Formation and other organic-rich rocks as suggested source contributors to petroleum formation. *Am. Ass. Petr. Geol. Bull.*, v. 68, pp. 1879-1893, Tulsa.

Received May 2, 1995; accepted July 18, 1995